Changes in correlation between spontaneous activity of dorsal horn neurones lead to differential recruitment of inhibitory pathways in the cat spinal cord

D. Chávez[1], E. Rodríguez[1,2], I. Jiménez[1] and P. Rudomin[1]

[1]Department of Physiology, Biophysics and Neurosciences, Centre for Research and Advanced Studies, National Polytechnic Institute, México DF, México
[2]Centre for Research in Mathematics, Autonomous University of Hidalgo, Hidalgo, México

The Journal of Physiology

Key points

- We have examined the functional organization of the neuronal ensembles involved in the generation of spontaneous cord dorsum potentials in the lumbo-sacral spinal cord of the anaesthetized cat.
- These potentials appear synchronously along several spinal segments and are generated by a longitudinally distributed network of bilaterally interconnected sets of dorsal horn neurones.
- Low levels of synchronization of spontaneous neuronal activity within this network appear associated with activation of spinal pathways mediating glycinergic non-reciprocal postsynaptic inhibition of motoneurones.
- During states of spontaneous increased synchronization, or after the acute section of cutaneous nerves, there is a preferential activation of the GABAergic pathways producing primary afferent depolarization and presynaptic inhibition of muscle and cutaneous afferents.
- It is suggested that modulation of the temporal synchronization of spontaneous activity of dorsal horn neurones might provide means for selection of alternatively operating inhibitory spinal pathways during different sensory and motor behaviours.

Abstract Simultaneous recordings of cord dorsum potentials along the lumbo-sacral spinal cord of the anaesthetized cat revealed the occurrence of spontaneous synchronous negative (n) and negative–positive (np) cord dorsum potentials (CDPs). The npCDPs, unlike the nCDPs, appeared preferentially associated with spontaneous negative dorsal root potentials (DRPs) resulting from primary afferent depolarization. Spontaneous npCDPs recorded in preparations with intact neuroaxis or after spinalization often showed a higher correlation than the nCDPs recorded from the same pair of segments. The acute section of the sural and superficial peroneal nerves further increased the correlation between paired sets of npCDPs and reduced the correlation between the nCDPs recorded from the same pair of segments. It is concluded that the spontaneous nCDPs and npCDPs are produced by the activation of interconnected sets of dorsal horn neurones located in Rexed's laminae III–IV and bilaterally distributed along the lumbo-sacral spinal cord. Under conditions of low synchronization in the activity of this network of neurones there would be a preferential activation of the intermediate nucleus interneurones mediating Ib non-reciprocal postsynaptic inhibition. Increased synchronization in the spontaneous activity of this ensemble of dorsal horn neurones would recruit the interneurones mediating primary afferent depolarization and presynaptic inhibition and, at the same time, reduce the activation of pathways mediating Ib postsynaptic inhibition. Central control of the synchronization in the spontaneous activity of dorsal horn neurones and its modulation by cutaneous inputs is envisaged as an effective

mechanism for the selection of alternative inhibitory pathways during the execution of specific motor or sensory tasks.

Corresponding Author P. Rudomin: Department of Physiology, Biophysics and Neurosciences, Centro de Investigación y de Estudios Avanzados del Instituto Politécnico Nacional, Av. Instituto Politécnico Nacional 2408, México DF 07360, México. Email: rudomin@fisio.cinvestav.mx

Abbreviations CDP, cord dorsum potential; DRP, dorsal root potential; IFP, intraspinal field potential; nCDP, negative cord dorsum potential; npCDP, negative–positive cord dorsum potential; PAD, primary afferent depolarization; SP, superficial peroneal; SU, sural.

Introduction

The identification and functional characterization of the last order interneurones mediating the GABAergic depolarization of the intraspinal terminals (PAD) of cutaneous and muscle afferents is essential for a better understanding of the role of presynaptic inhibition in motor performance and sensory integration. By examining PAD elicited monosynaptically in sensory fibres by intraspinal microstimulation, Jankowska *et al.* (1981) concluded that the last-order interneurones mediating the PAD of muscle and cutaneous afferents are located within the intermediate zone and dorsal horn, respectively. Averaging of dorsal and ventral root potentials triggered by the action potentials of single interneurones located within the intermediate zone disclosed two main classes of interneurones (Rudomin *et al.* 1987; Rudomin, 1990). The action potentials of Class I interneurones were associated with short latency inhibitory potentials in motoneurones, in contrast with the activity of Class II interneurones that was generated in synchrony with dorsal root potentials (DRPs) and inhibitory potentials in motoneurones. Subsequent work led to the proposal that Class I interneurones mediate the non-reciprocal Ib glycinergic postsynaptic inhibition exerted on motoneurones, while Class II interneurones mediate the GABAergic PAD of group I afferents and also GABAergic inhibitory actions in motoneurones (Rudomin *et al.* 1990).

Spike triggering averaging procedures revealed that the spontaneous action potentials of Class I and Class II interneurones were preceded by relatively slow (50–100 ms) negative cord dorsum potentials (CDPs), and it was assumed that these CDPs were generated by the spontaneous activation of two different populations of dorsal horn neurones, one driving Class I and the other Class II interneurones (see Rudomin *et al.* 1987, 1990). Further studies indicated that dorsal horn neurones firing in synchrony with these spontaneous CDPs also responded with mono- or with oligosynaptic latencies to electrical stimulation of low-threshold cutaneous afferents. This was consistent with the finding that during the generation of the spontaneous CDPs, transmission along the pathways producing PAD of muscle and cutaneous afferents was affected in the same manner as by electrical stimulation of cutaneous nerves (Manjarrez *et al.* 2000).

Subsequent work indicated that spontaneous CDPs appear synchronized along the lumbo-sacral enlargement, being largest in the L5 and L6 segments (Manjarrez *et al.* 2000; García *et al.* 2004). Although the intersegmental synchronization between spinal cord potentials appears to arise from intrinsic spinal cord mechanisms (Kerkut & Bagust, 1995; Lidierth & Wall, 1996; García *et al.* 2004), there is limited information on the extent to which this synchronization depends on or is modified by sensory and supraspinal influences.

Rudomin *et al.* (1987) observed that quite often the action potentials of Class I interneurones appeared associated with spontaneous negative CDPs (nCDPs) and those of Class II interneurones with negative–positive CDPs (npCDPs). Even so, Manjarrez *et al.* (2000, 2003) used spontaneous CDPs exceeding preset amplitudes to examine the functional organization of the neuronal ensembles involved in their generation. This prevented disclosure of possible differences in the organization of the neuronal ensembles involved in the generation of spontaneous nCDPs and npCDPs. To approach this issue, we have now used a specially designed computer program to select the spontaneous CDPs recorded in one segment (usually L5 or L6) either as nCDPs or npCDPs. These potentials were taken as reference to retrieve the spontaneous CDPs generated simultaneously in different spinal segments (see García *et al.* 2004). This allowed measurements of the correlation between paired sets of nCDPs or npCDPs as well as their possible relation with spontaneous DRPs and the effects produced on them by the acute section of cutaneous nerves in preparations with intact neuroaxis and after spinalization.

The present observations support the proposal that the neurones involved in the generation of the spontaneous nCDPs and npCDPs are organized as a network of interconnected sets of dorsal horn neurones bilaterally distributed along the lumbo-sacral spinal cord. Under conditions of low synchronization, there would be a preferential activation of the intermediate nucleus interneurones mediating Ib non-reciprocal postsynaptic inhibition. Increased synchronization in the spontaneous activity of this ensemble of dorsal horn neurones would recruit the interneurones mediating primary afferent depolarization and presynaptic inhibition and at the same

time reduce the activation of pathways mediating Ib postsynaptic inhibition. A preliminary account of some of the results has been presented (Rudomin, 2009).

Methods

Ethical approval

All experiments were approved by the Institutional Ethics Committee for Animal Research (Protocol no. 126-03) and comply with the ethical policies and regulations of *The Journal of Physiology* (Drummond, 2009) and of the National Institutes of Health (Bethesda, MD, USA; Animal Welfare Assurance no. A5036-01). The *Guide for the Care and Use of Laboratory Animals* (National Research Council, 2010) was followed in all cases.

General procedures

The experiments were carried out in 15 young adult cats of either sex. The animals were initially anaesthetized with pentobarbitone sodium (40 mg kg^{-1} I.P.). The carotid artery, radial vein, trachea and urinary bladder were cannulated. Additional doses of pentobarbitone sodium (5 mg kg^{-1} h^{-1}) were given intravenously to maintain an adequate level of anaesthesia, tested by assessing that withdrawal reflexes were absent, that the pupils were constricted and that arterial blood pressure was between 100 and 120 mmHg. A solution of 100 mM of sodium bicarbonate with 5% glucose was given I.V. (0.03 ml min^{-1}) to prevent acidosis (Rudomin *et al.* 2007). When necessary, 10% dextran or ethylephrine (Effortil, Boering-Ingelheim) was administered to keep blood pressure above 100 mmHg.

The lumbo-sacral and low thoracic spinal segments were exposed by laminectomy and opening of the dura mater. The left sural (SU) and superficial peroneal (SP) nerves were dissected free and kept in continuity. After the surgical procedures, the animals were transferred to a stereotaxic metal frame allowing immobilization of the head and spinal cord, subject to neuromuscular blockade with pancuronium bromide (0.1 mg kg^{-1}) and artificially ventilated. The tidal volume was adjusted to maintain 4% of CO_2 concentration in the expired air. To prevent desiccation of the exposed tissues, pools were made with the skin flaps, filled with paraffin oil and maintained between 36 and 37°C by means of radiant heat.

Recordings and stimulation

Usually six ball electrodes were placed on the cord dorsum of the lumbo-sacral enlargement in different spinal segments to record spontaneous and evoked cord dorsum potentials (CDPs), each of them against an indifferent electrode placed on nearby paravertebral muscles. Electrodes placed on the cord dorsum along the same side of the spinal cord were separated between 7 and 10 mm. Separation between the left and right electrodes in the L6 and L5 segments varied between 3 and 4 mm.

Intraspinal field potentials (IFPs) were recorded with glass micropipettes (1–2 MΩ, 2–3 μm tip diameter) filled with a 2 M solution of NaCl. These electrodes were placed in the middle L6 segment. They were inserted vertically in the rostro-caudal direction with an angle of 5–7 deg in the transverse plane. In several experiments a small filament of the left L6 dorsal root was in addition dissected, sectioned and its central end placed on a pair of Ag–AgCl electrodes to record dorsal root potentials (DRPs). The intact SU and SP nerves were mounted on bipolar hook electrodes for stimulation. Stimulus strength is expressed as multiple of the minimum strength required to produce detectable afferent volleys in the cord dorsum by nerve stimulation (threshold, *T*).

Acute nerve and spinal lesions

Some experiments involved acute transection of the left SP, SU or sciatic nerve and lumbo-sacral dorsal roots in both sides of the spinal cord. Complete spinal cord transections were performed at low thoracic level (T10) under a dissecting microscope using a fine pair of tweezers. Care was taken not to move the spinal cord and the surface recording electrodes.

Data processing

Spontaneous and cutaneous-nerve evoked CDPs, IFPs and DRPs were recorded with separate preamplifiers (band pass filters 0.3 Hz to 10 kHz), displayed on an oscilloscope, digitized with a sampling rate of 10 kHz and stored in computer disc memory for subsequent processing.

After the experiment, the spontaneous CDPs recorded in one (reference) segment that exceeded a predetermined amplitude ($>5 \mu$V) were sequentially displayed and aligned using a peak detection program (see below). Negative potentials that emerged from a relatively flat baseline and lasted 40–60 ms were considered as nCDPs (see Figs 1*B* and 5*B*, upper traces), and negative potentials that were followed by a slow positive wave lasting 50–70 ms were considered as npCDPs (see Fig. 5*C* upper traces).

The selected nCDPs and npCDPs (usually 30–40) were stored in separate files. Their means, plus and minus a specified range (±20–30% of mean), were used afterwards as templates to retrieve the 'reference' nCDPs and npCDPs generated during the whole recording period (usually 20–30 min to have sufficient samples for further analysis). With this method the largest and smallest reference CDPs (around 15–20% of the whole sample) were excluded from
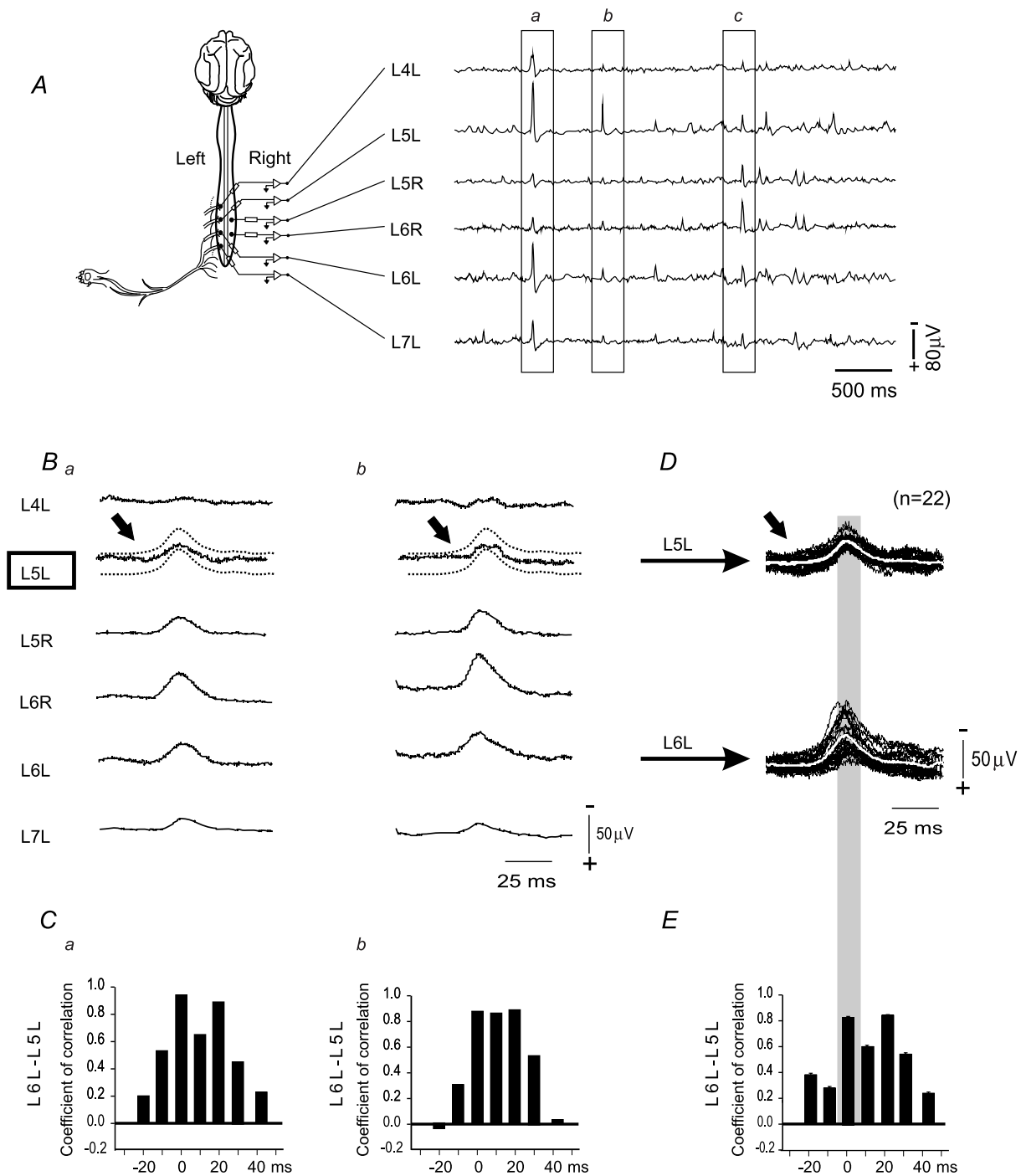
Figure 1. Diagram of the method
A, six ball electrodes were placed on the cord dorsum, four on the left side on lumbar segments L4–L7 and two on the right side in segments L5 and L6, as indicated. Traces show the spontaneous cord dorsum potentials recorded from these segments. *Ba* and *b*, two sets of spontaneous CDPs simultaneously recorded in different spinal segments selected using as reference the L5L nCDPs (indicated by arrows). Template selection range (±30% of mean) is shown by dotted traces above and below the L5L CDPs. *C*, coefficients of correlation between the L5L reference nCDPs and the associated L6L CDPs, calculated for different 10 ms time windows. *D*, superposed L5L and L6L CDPs and their means (white traces). *E*, median and standard errors of coefficients of correlation between the L5L and L6L CDPs obtained from 22 sets of potentials similar to those illustrated in *Ba* and *Bb*. Note that the coefficients of correlation increase during the CDPs. Shaded bar in *D* and *E* set at the time of the peak of the CDPs. In all figures negativity is upwards for the CDPs. See text for further details.

the selection procedure, leaving sets of reference CDPs of similar shape and amplitude. Visual inspection of the collected CDPs was made to remove potentials that could not be clearly classified as nCDPs or npCDPs.

Coefficients of correlation

Analysis of the fluctuations of the cord dorsum potentials recorded from a single site provided limited information pertaining to the functional organization of the neuronal networks involved in the generation of these potentials. Therefore we focused on the analysis of the correlated fluctuations of the CDPs recorded from different spinal segments that were estimated with the coefficient of correlation (CC). The most familiar measure of dependence between two quantities is the Pearson product–moment correlation coefficient, and has been used in previous studies (Rudomin *et al.* 1969). It is obtained by dividing the covariance of the two variables by the product of their standard deviations. The population correlation coefficient $\rho_{X,Y}$ between two random variables X and Y with expected values μ_X and μ_Y and standard deviations σ_X and σ_Y is defined as:

$$\rho_{x,y} = \mathrm{corr}(X, Y) = \mathrm{cov}(X, Y)/\sigma_x\sigma_y$$
$$= E\left[(X - \mu_x)(Y - \mu_y)\right]/\sigma_x\sigma_y$$

Figure 1*Ba* and *b* shows two sets of spontaneous CDPs simultaneously recorded from several spinal segments, as indicated. These potentials were retrieved using as reference the nCDPs recorded in the L5L segment, selected by means of the template (shown by the dotted traces above and below the CDPs marked with the arrow). To calculate the correlation between the L5L and L6L CDPs (nCDPs in this case), the data were divided in 7–10 successive time windows of 10 ms each, starting about 30 ms before the peak of the CDPs. Since the sampling rate was of 10 kHz, each window included 100 data points.

The histograms in Fig. 1*Ca* and *b* display the coefficients of correlation calculated for each set of time windows before and during the CDPs. These histograms show that the highest correlations occurred around the peak of the nCDPs. For a given time window, the CCs calculated for all the pairs of CDPs in the sample had a skewed distribution. Therefore, instead of the mean correlation, we calculated the median and its standard error, as shown in Fig. 1*E*. To compare changes produced by the different experimental procedures we used the CCs obtained from windows set at the time of the peak of the CDPs (see shaded column in Fig. 1*D* and *E*). The level of significance between pairs of CCs was assessed with Wilcoxon's signed-rank test implemented in MATLAB (The Mathworks, Inc., Natick, MA, USA). The obtained values ($P < 0.01$, $P < 0.05$ and $P < 0.10$) are indicated in the corresponding figures.

Histology

At the end of the experiment the animal was euthanized with a pentobarbital overdose and perfused with 10% formalin; the spinal cord was removed, leaving the recording micropipettes in place. After fixation and dehydration, the spinal cord segment containing the recording micropipette was placed in a solution of methyl salicylate for clearing. Subsequently, the spinal cord was cut transversely to obtain sections containing the recording micropipette. The tracks left by the micropipette were drawn with a camera lucida (Wall & Werman, 1976). A tissue shrinkage factor of 10% was assumed in localizing the lamina, and the validity of this factor was verified by measuring distances between identified electrode tracks.

Results

Segmental distribution of the spontaneous CDPs

Simultaneous recordings from the cord dorsum in the lumbo-sacral enlargement revealed spontaneous potentials of different shapes and amplitudes. The most prominent potentials were usually negative (nCDPs) or negative–positive (npCDPs). The negative components of these potentials lasted 40–60 ms and had peak amplitudes between 5 and 100 μV. They could appear in one segment only or be synchronized in several segments, either on one side of the spinal cord or bilaterally. Figure 1*A* shows the spontaneous CDPs simultaneously recorded in one experiment with six ball electrodes, four of them placed on the cord dorsum in the middle of the L4–L7 segments on the left side and two on the L5 and L6 segments in the right side, as indicated in the diagram.

The amplitudes and segmental distribution of these spontaneous CDPs was quite variable. At one time the CDPs recorded on the left side of the spinal cord were significantly larger than those recorded in the right side of the same segment (as in box *a* of Fig. 1*A*), but shortly after, a different pattern of CDPs emerged. Namely, the CDPs recorded in the L5 segment on the left side were larger than the potentials recorded in all the other segments (box *b*). Later on, simultaneous CDPs appeared in all segments, but the CDPs recorded from the right side were larger than those recorded from the left side (box *c*).

Particular combinations of spontaneous CDPs could be observed several times during a single recording period, suggesting they were not generated by a random process, as was subsequently verified by fractal analysis, but reflected a finite number of repeatable patterns (Rodríguez *et al.* 2010, 2011).

The segmental distribution and variability of the spontaneous CDPs recorded in different segments depended, to a great extent, on the site selected to record

the reference CDPs. The traces depicted in Fig. 2*A* show the CDPs retrieved when using as reference the nCDPs recorded in the left L5 segment (L5L, arrow). Figure 2*B* shows instead the potentials retrieved using as reference the nCDPs recorded in the right L5 segment (L5R arrow) and Fig. 2*C* and *D* the CDPs obtained when using as

reference the nCDPs recorded in the left and right L6 segments (L6L and L6R, respectively).

The boxes on the upper right side of each set of recordings in Fig. 2*A–D* show the segmental distribution of the coupling ratios obtained by dividing the mean peak amplitude of the associated nCDPs by the mean
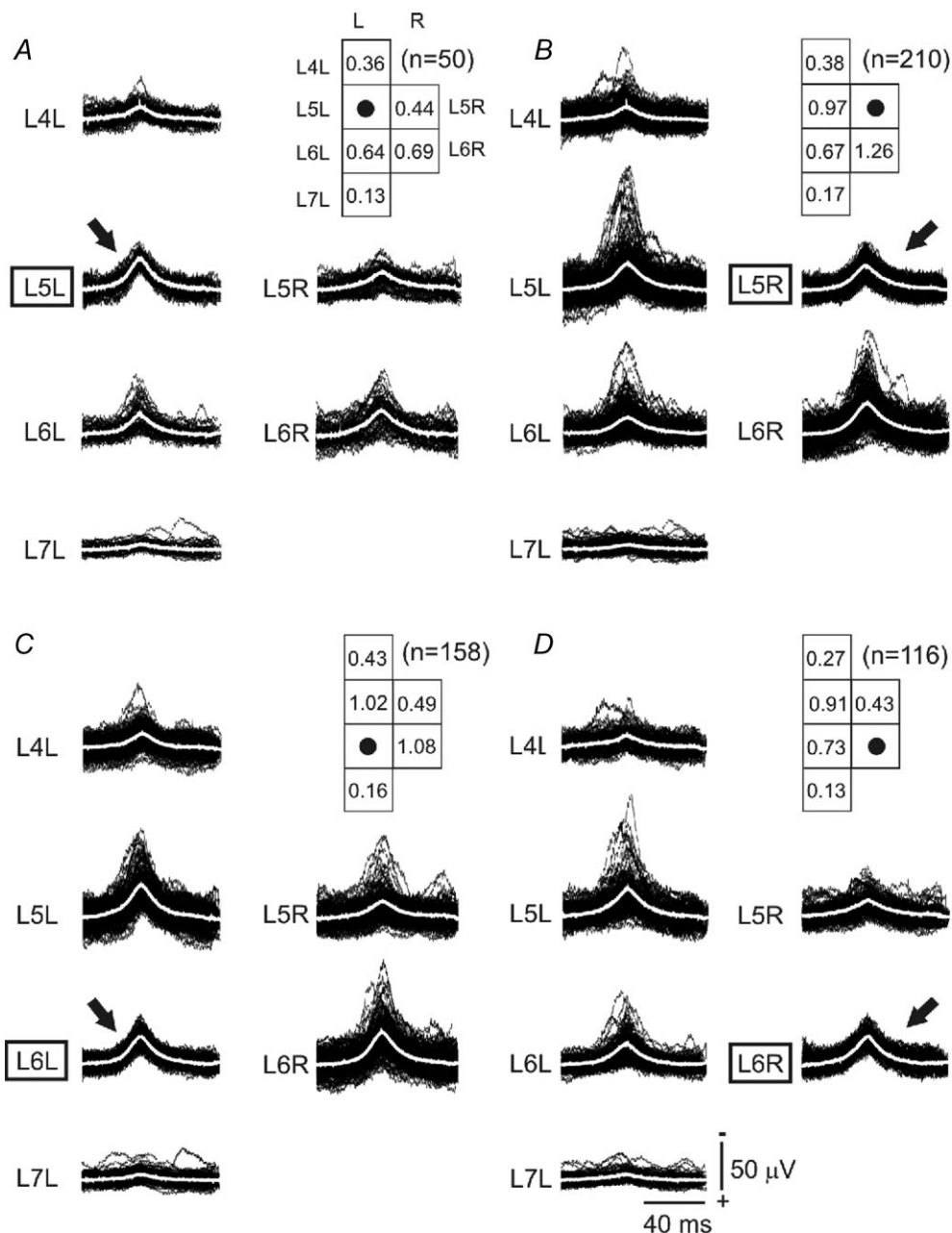

Figure 2. Spontaneous CDPs selected using reference potentials from different spinal segments
A–D, spontaneous nCDPs recorded in a given segment were selected by means of a predetermined template and used as reference (shown by arrows) to display the potentials occurring at the same time in other segments (associated CDPs), as indicated. This procedure displayed synchronized potentials in the left as well as in the right sides of the spinal cord. Each panel shows superposed traces and means (white traces). The boxes on the right side of each set of recordings show the coupling ratios obtained by dividing the mean peak amplitude of the associated CDPs by the mean peak amplitude of the reference nCDPs (their segmental location is marked with a circle). Number of samples is indicated in parentheses. Further explanations in text.

peak amplitude of the reference nCDPs (location marked with a circle in the boxes). It may be seen in Fig. 2*A* that although the mean peak amplitude of the L5R nCDPs was 0.44 relative to the mean peak amplitude of the reference L5L nCDPs, the fluctuations of the potentials were similar to those of the reference nCDPs. In contrast, when using as reference the L5R nCDPs (Fig. 2*B*), the L5L nCDPs had about the same mean peak amplitude as the reference CDPs (ratio 0.97) but the individual potentials showed rather large fluctuations. The asymmetry in the fluctuations was also evident when comparing the L5L nCDPs associated with the L6L reference nCDPs (Fig. 2*C*) or with the L6R reference nCDPs (Fig. 2*D*). Similar results have been obtained in four other experiments when using as reference the nCDPs as well as the npCDPs (not illustrated). These observations suggest that using as reference the CDPs recorded in a specific segment allows selection of a particular set of neurones which can be different from those sets selected when using as reference the CDPs recorded in other segments (see Discussion).

It is possible that the ball electrodes used to record the cord dorsum potentials picked up, in addition to potentials generated locally, potentials generated at some distant source. This situation could be particularly important when dealing with the correlation between CDPs recorded with closely placed electrode pairs. Although we cannot completely exclude recording of common potentials by closely placed electrodes, simultaneous recordings of the CDPs generated in adjacent segments support the view that, at least in some cases, the recorded CDPs were generated locally.

One example of this situation is illustrated in Fig. 3. In this experiment we recorded spontaneous CDPs from four segments in the left side (L4–L7) and from two segments in the right side (L5 and L6). The CDPs depicted in Fig. 3*A* were retrieved using as reference the spontaneous nCDPs recorded in the left L5 segment (see arrow). The CDPs were separated in different groups according to their patterns of segmental distribution, five in this case (Fig. 3*B*). Two of them showed synchronized spontaneous CDPs in all segments (Fig. 3*Ba* and *b*). The three sets illustrated in Fig. 3*Bc–e*, were clearly different from those depicted in Fig. 3*Ba* and *b*, because rather small or no spontaneous CDPs were recorded from the right side in the L5 segment, even though the reference potentials recorded in the left side were of about the same size as those illustrated in Fig. 3*Ba* and *b*.

Similar findings were obtained with sets of CDPs associated with the reference L5L npCDPs (Fig. 3*C*). In this case the retrieved CDPs showed four different patterns (Fig. 3*D*). In one of them CDPs appeared synchronized in all segments (Fig. 3*Da*). The other three showed reference L5L npCDPs with rather small or no associated L5R CDPs (Fig. 3*Db–d*).

Although the spontaneous CDPs recorded from the left and right side in the L6 segment were more correlated than the L5L and L5R CDPs, some of the observed patterns also suggested a local origin of the CDPs. For example, in Fig. 3*Ba* the L6R CDPs were twice the amplitude of the L6R CDPs displayed in Fig. 3*Bc*, even though the L6L CDPs were in both cases of about the same amplitude. On the other hand, L6L CDPs of similar amplitudes could appear associated either with relatively large (Fig. 3*Da*) or with small L6R CDPs (Fig. 3*Dc*).

Additional support for a local origin of the CDPs is provided by the opposite effects produced by SU and SP nerve section on the correlation between paired sets of nCDPs and of paired sets of npCDPs (see below).

Correlation between spontaneous cord dorsum and dorsal root potentials

Stimulation of the most excitable fibres in a cutaneous nerve produces negative–positive fields in the dorsal horn. The negative component has been attributed to mono-synaptic activation of dorsal horn neurones and the positive component to the current flows generated during PAD (Eccles, 1963). On this basis, we hypothesized that the spontaneous DRPs would appear preferentially associated with the npCDPs rather than with nCDPs. Preliminary observations suggested that this could be the case (see Rudomin, 2009). However, no tests were made at that time to assess the selectivity of the procedures used to retrieve the reference nCDPs and npCDPs (see Methods). Therefore, a new series of observations was performed to examine with more detail the correlation between the spontaneous DRPs and the nCDPs and npCDPs.

Figure 4 illustrates results obtained in one experiment. The spontaneous CDPs recorded in the L4L and L5L segments, as well as the DRPs retrieved by using as reference the nCDPs recorded in the L6L segment are displayed in Fig. 4*A*. Twelve out of the 36 selected sets of L6L-nCDPs and associated DRPs are displayed in Fig. 4*B*. These sets were separated in three groups. Figure 4*Ba* shows three cases in which the L6L nCDPs were clearly associated with a slightly positive DRP, while Fig. 4*Bb* and *c* shows several cases where no synchronized potentials appeared in the dorsal root recordings. In the experiment of Fig. 4 not all of the potentials selected using as reference the L6L nCDPs were purely negative. In some records ($n = 3$) the negative component was followed by a small positivity (see CDP marked with an asterisk in Fig. 4*Bb*). But even so, only one of the 36 nCDPs (2.8%) appeared to be associated to a small negative DRP attributable to PAD.

The spontaneous CDPs as well as the DRPs retrieved when using as reference the L6L npCDPs are displayed in Fig. 4*C*. It is to be noted that in this case the mean DRPs showed a distinct negative component attributable

to PAD. Figure 4*D* displays individual sets of L6L npCDPs and their associated DRPs. The recordings depicted in Fig. 4*Da* show the negative component of the CDPs followed by a relatively large positivity. All these potentials appeared associated with distinct negative DRPs. The npCDPs displayed in Fig. 4*Db* had instead a smaller positive component, but even so they were all associated to negative DRPs. Finally, Fig. 4*Dc* shows several npCDPs that occurred together with relatively small or no negative DRPs, in some cases preceded by a positive component.
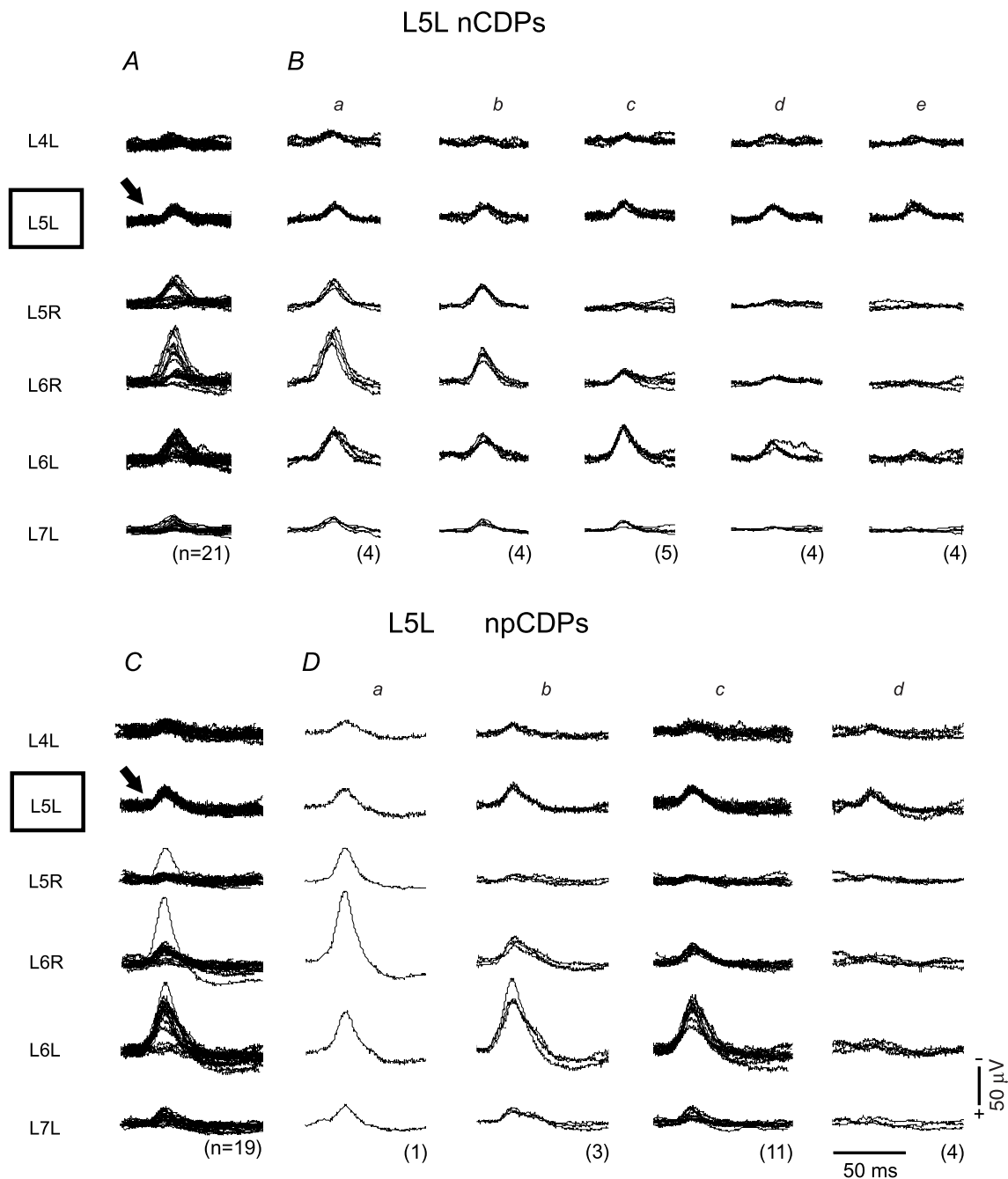

Figure 3. Segmental patterns of spontaneous CDPs
A, spontaneous CDPs recorded from different spinal segments occurring in association with the L5L nCDPs (see arrow). *Ba–e*, CDPs displayed in *A* separated according to their patterns of segmental distribution. *C* and *D*, as *A* and *B*, for potentials retrieved using as reference the L5L npCDPs. Number of samples is indicated in parentheses. Further explanations in text.

Disclosure of the individual components of the reference L6L npCDPs, partly displayed in Fig. 4*D*, indicated that only 1 out of 28 CDPs (3.5%) had no positive phase. Yet, a DRP with a small negative component appeared synchronized with the npCDP (marked with asterisk in Fig. 4*Db*). Similar results were obtained in another three experiments using as reference the CDPs recorded from the left L6 segment while recording the DRPs from a left dorsal rootlet in the same segment.

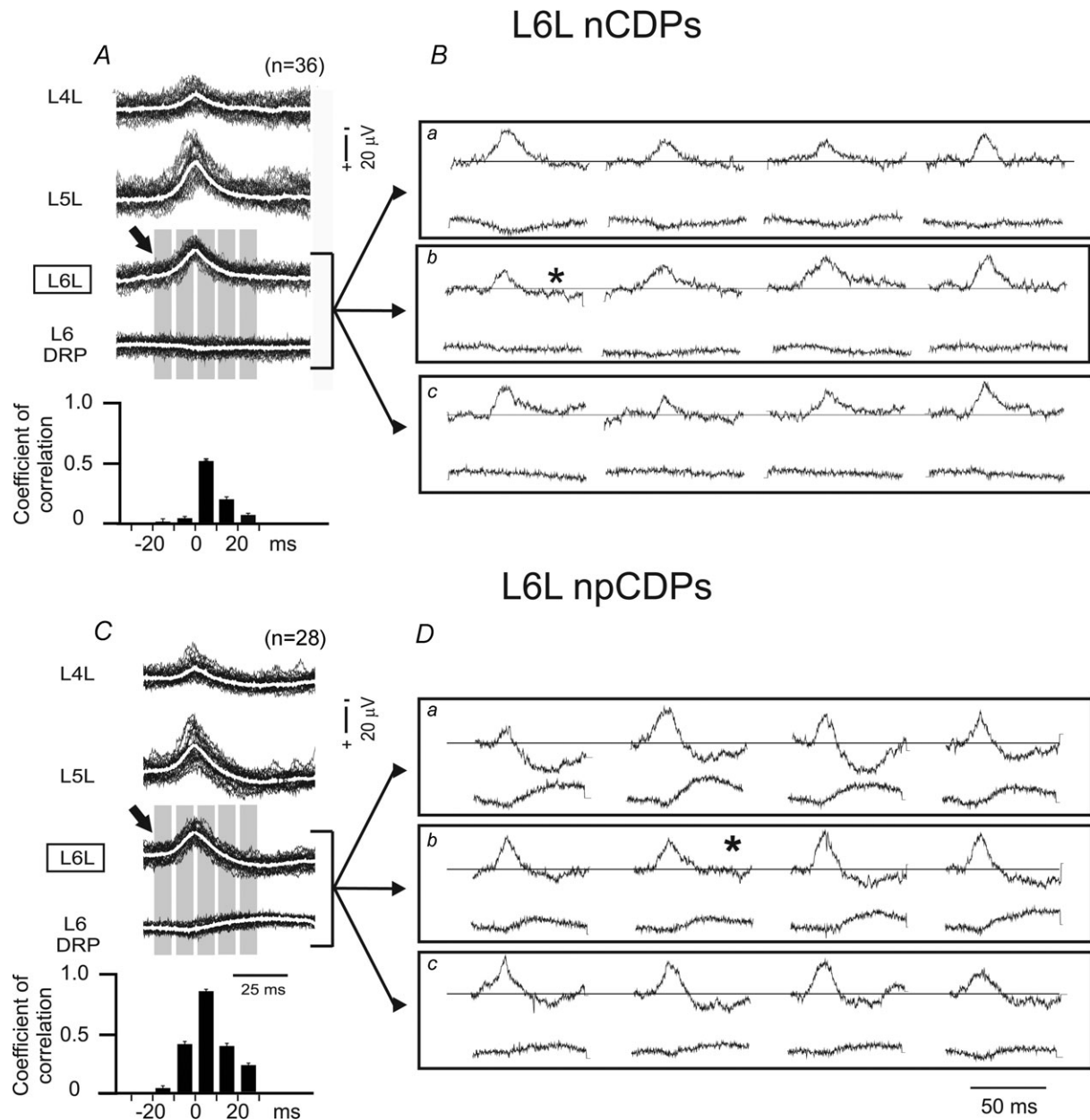To further evaluate the possible association of PAD with the npCDPs, we examined the correlation between the

Figure 4. Spontaneous DRPs appear preferentially associated with npCDPs
Simultaneous recordings were made from the left L4, L5 and L6 segments in the cord dorsum and from the central end of a small L6 dorsal rootlet in the same side. *A*, spontaneous CDPs and DRPs retrieved using as reference the L6L nCDPs (see arrow). *B*, examples of individual L6L nCDPs and associated DRPs displayed in *A* separated in 3 different groups. Note that the DRPs displayed in panel *a* show a positive component only. In panels *b* and *c*, no DRPs appear associated with nCDPs. Histogram in *A* shows the median and standard error of the coefficients of correlation between the L6L CDPs and the DRPs calculated using 10 ms time windows (marked with grey bars in *A*). *C* and *D* the same as in *A* and *B*, but for CDPs and DRPs retrieved using as reference the L6L npCDPs. Further explanations in text.

individual DRPs and L6L nCDPs or npCDPs. We used five time windows of 10 ms each to calculate the coefficient of correlation for each paired set. As shown by the grey columns in Fig. 4*A* and *C*, two time windows were placed before the peak of the negative component of the CDPs and three after the peak. This procedure was applied to each pair of CDPs and DRPs (such as those illustrated in Fig. 4*B* and *D*). Thereafter we calculated the median and standard errors of the whole set of data. The obtained values are displayed as histograms in the lower part of Fig. 4*A* and *C*.

It may be seen in these graphs that at the time of the peak of the nCDPs, the coefficient of correlation with the DRPs was relatively high (0.50 ± 0.02) probably because of the simultaneous occurrence of the positive component in the DRP recordings. However, the correlation between npCDPs and DRPs calculated at a similar time interval was significantly higher (0.84 ± 0.01; $P < 0.01$). The correlation measured at later times, already during the negative component of the DRPs, was also higher.

Comparable differences were observed in two other experiments. In one of them, the coefficient of correlation between the L6L nCDPs calculated at the time of the peak of the negative component and the DRPs was 0.44 ± 0.04 while the coefficient of correlation between the npCDPs and DRPs at the same time interval was 0.74 ± 0.01. In the third experiment we obtained values of 0.55 ± 0.02 and of 0.78 ± 0.01, respectively. The observed differences were also statistically significant ($P < 0.01$).

These observations further support the proposal that in contrast with the spontaneous nCDPs, the spontaneous npCDPs are preferentially associated with negative DRPs, which are indicators of PAD.

Intraspinal distribution of nCDPs and npCDPs

Recordings such as those depicted in Fig. 3 indicated that the interneurones involved in the generation of the nCDPs and npCDPs had a similar segmental distribution. However, it was not clear if these potentials were generated by interneurones located within the same or within different spinal layers. We hypothesized that these sets of neurones would have a similar intraspinal distribution within the dorsal horn. Figure 5 illustrates the results obtained in one experiment where we performed a detailed mapping of the intraspinal field potentials (IFPs) associated with the reference L6L nCDPs and npCDPs. Spontaneous and evoked IFPs were recorded at different depths in four vertical tracks separated by 400 μm (see arrows in Fig. 5*D*).

The mean IFPs produced by electrical stimulation of the SP nerve (single pulses, $1.3T$ strength) recorded at different depths are shown in Fig. 5*A*. These potentials were recorded along one of the four microelectrode tracks (marked with asterisk in Fig. 5*D*). It may be seen that these IFPs were negative in the superficial layers, attained their maximal amplitude at 1.6 mm depth relative to the surface of the spinal cord, and reversed their polarity between 2.0 and 2.6 mm depth. As shown by the contour map of Fig. 5*D*, obtained from the SP-evoked IFPs recorded along the four microelectrode tracks, the zone of maximal negativity was located in the dorsal horn, in what appears to be the middle and lateral parts of Rexed's laminae III and IV (see Jankowska *et al.* 1981 and Manjarrez *et al.* 2000).

Figure 5*B* shows the spontaneous IFPs associated with the reference L6L nCDPs. These IFPs were recorded at different depths in the same track as above. They were also negative in the most superficial layers and were largest between 1.2 and 1.6 mm depth. Like the SP-evoked IFPs, they reversed their polarity between 2.0 and 2.6 mm depth. As shown by the isopotential contours, the region of maximal negativity was also within Rexed's laminae III–IV, slightly more dorsal to the region of SP projection (Fig. 5*E*).

The IFPs associated with the L6L npCDPs are illustrated in Fig. 5*C*. These npIFPs were also positive–negative in the most superficial spinal layers, and had practically the same intraspinal distribution as the spontaneous nIFPs associated to the nCDPs (Fig. 5*C* and *F*).

As initially hypothesized, these observations indicate that the neuronal ensembles involved in the generation of the nCDPs and the npCDPs are not spatially segregated, but are located within the same dorsal horn regions where large SP afferents project.

Segmental synchronization of CDPs

The purpose of these experiments was to test the hypothesis that the intersegmental synchronization between the spontaneous CDPs basically results from intrinsic spinal mechanisms, which are in turn modulated by supraspinal and segmental activity.

Based on our previous suggestion that pathways mediating PAD are subjected to stronger correlating inputs than pathways mediating Ib postsynaptic inhibition (Rudomín *et al.* 1987), an additional working hypothesis was that paired sets of spontaneous npCDPs recorded from different segments would have a higher correlation than the nCDPs.

To test these proposals we first examined the extent to which the magnitude of the correlation depended on the segmental location of the reference and associated CDPs and whether there were some differences in the correlation between paired sets of nCDPs and npCDPs retrieved from different segmental locations.

In the experiment of Fig. 6 the CDPs recorded in several segments were retrieved using as reference the L6L nCDPs.

While the neuroaxis was still intact, the coupling ratios of the L5L CDPs and of the L6R CDPs, relative to the reference L6L nCDPs, were 1.02 and 1.08, respectively (see boxes in Fig. 6*B*). Yet, their fluctuations were significantly larger, suggesting variable transmission along the involved pathways and/or variable recruitment of discrete neuronal aggregates. Similar findings were obtained for the npCDPs (not illustrated).

Figure 7*A* shows the segmental distribution of the coefficients of correlation measured at the time of the peak of the spontaneous CDPs selected using as reference the L5L nCDPs. These calculations were made using the potentials recorded in the same experiment as that of

Fig. 6. The ordinates indicate the different combinations of recording pairs and the abscissa the median and standard error of the coefficients of correlation (ρ) attained at the peak of the CDPs (see Fig. 1*E* and Methods). The obtained values are plotted as horizontal bars and displayed in decreasing order from above downwards. The different combinations of CDPs were separated in five groups according to the magnitude of their coefficients of correlation (ranges are indicated by the vertical lines in Fig. 7*A*). It is to be noted that the nCDPs recorded from adjacent segments (groups 2 and 3) had higher coefficients of correlation than nCDPs recorded from more distant pairs (group 4).
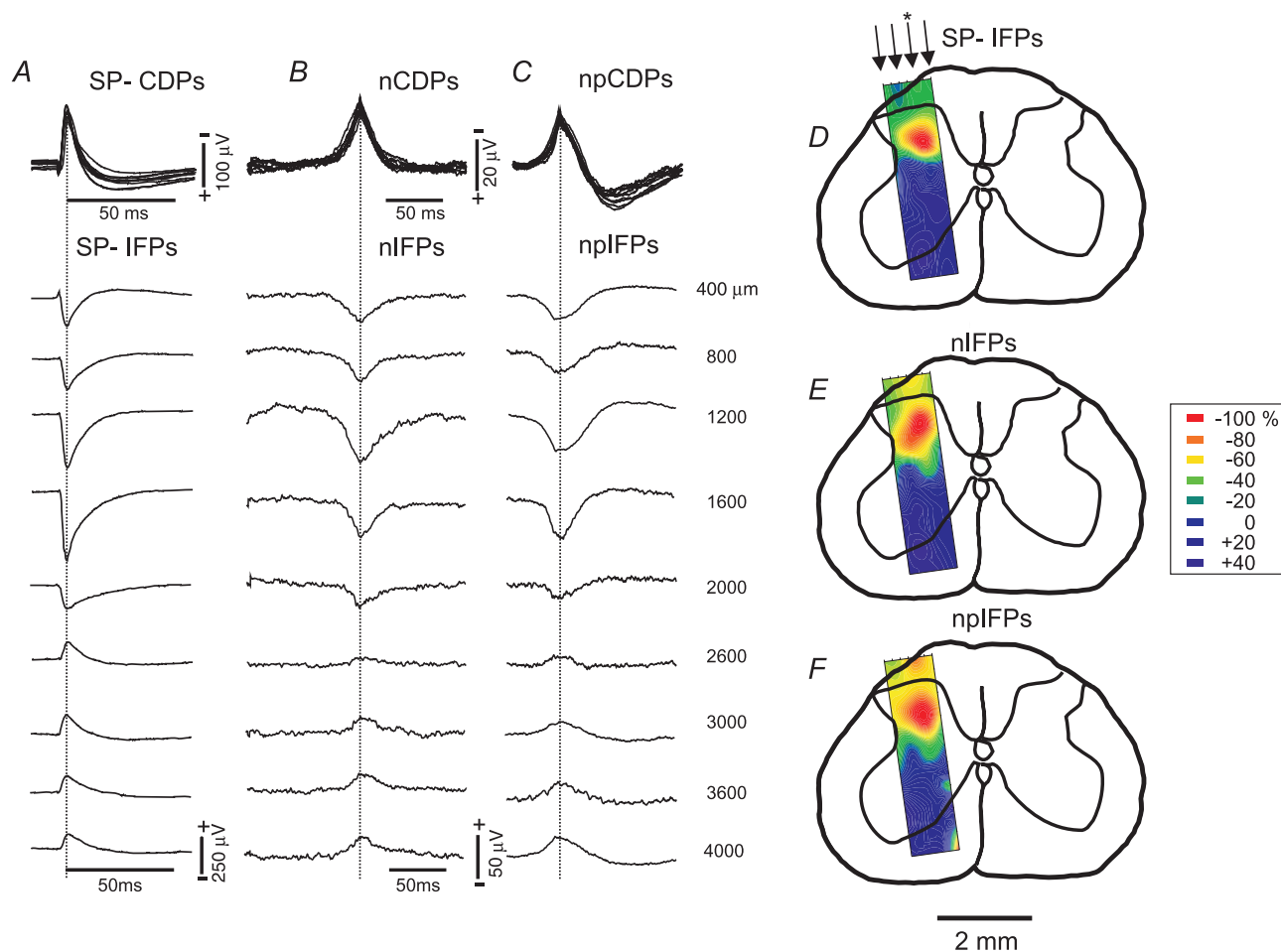

Figure 5. Intraspinal distribution of field potentials associated with spontaneous nCDPs and npCDPs
A, mean CDPs and intraspinal field potentials (IFPs) produced by electrical stimulation of the SP nerve with single pulses of 1.3*T* applied once every second. IFPs were recorded at different depths in a single electrode track (marked with asterisk in *D*). Means of the simultaneously recorded SP-CDPs have been superposed (upper set of traces). *B*, intraspinal distribution of spontaneous IFPs associated with reference L6L nCDPs; same microelectrode track as in *A*. Upper traces show the means of the reference L6L nCDPs used for IFP selection, one for each recording depth. *C*, same as *B*, but for IFPs associated with spontaneous L6L npCDPs. *D*, contour maps of SP evoked responses obtained using data collected from 4 microelectrode tracks (see arrows in *D*) superposed on drawing obtained from histology. *E*, contour maps of nIFPS (associated with nCDPs). *F*, contour maps obtained from npIFPS (associated with npCDPs). Voltage measurements made at time of maximal negativity of the CDPs (indicated by vertical lines in *A*, *B* and *C*). Negativity down for IFPs in *A*–*C*. In the contour maps of *D*–*F*, potentials were plotted as a percentage of the maximal amplitude of the negative components (see insert). Further explanations in text.

Figure 7*I* shows the distribution of the coefficients of correlation calculated for the pairs of CDPs retrieved by using as reference the L5L npCDPs, that is of those CDPs associated with the generation of PAD. The obtained correlations were displayed *keeping the same ordinates* as

in Fig. 7*A*. As expected, the coefficients of correlation between most combinations of npCDPs were higher than the combinations of nCDPs.

The coefficients of correlation depicted in Fig. 7*A* and *I* are presented as polar plots in Fig. 7*E* and *M*. To emphasize
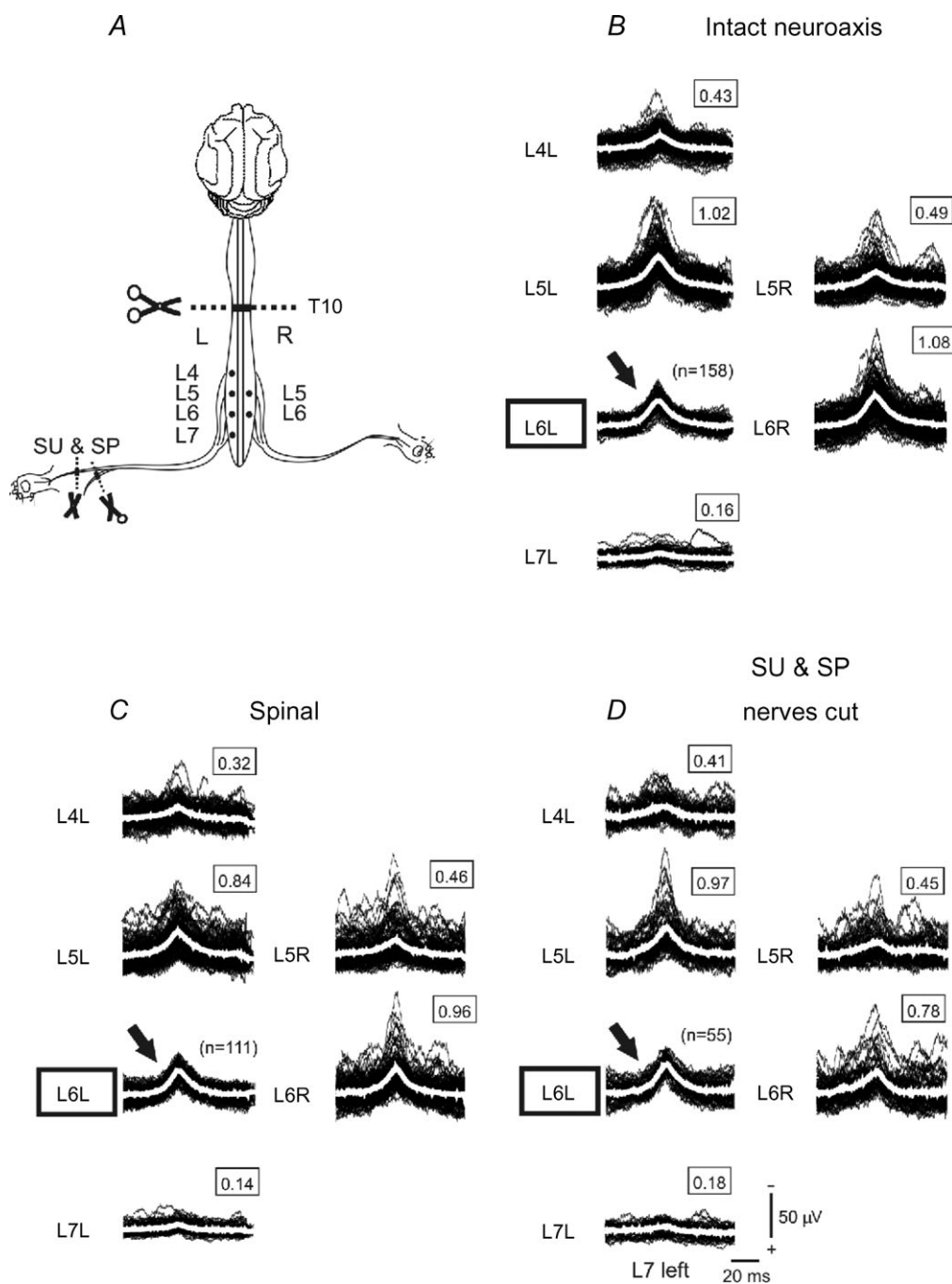

Figure 6. Effects of acute spinalization and cutaneous nerve transection on spontaneous nCDPs
Same format as that of Fig. 2. *A*, recording arrangement. *B*, intact neuroaxis. Superposed segmental CDPs retrieved using as reference the L6L nCDPs and their means (see arrow). *C*, recordings taken 20 min after acute spinalization at low thoracic level (T10). *D*, spontaneous nCDPs recorded 2 h after spinalization and 20 min after acute transection of the left SU and SP nerves. Numbers in boxes indicate mean peak amplitude ratios of CDPs relative to reference CDPs. Further explanations in text.
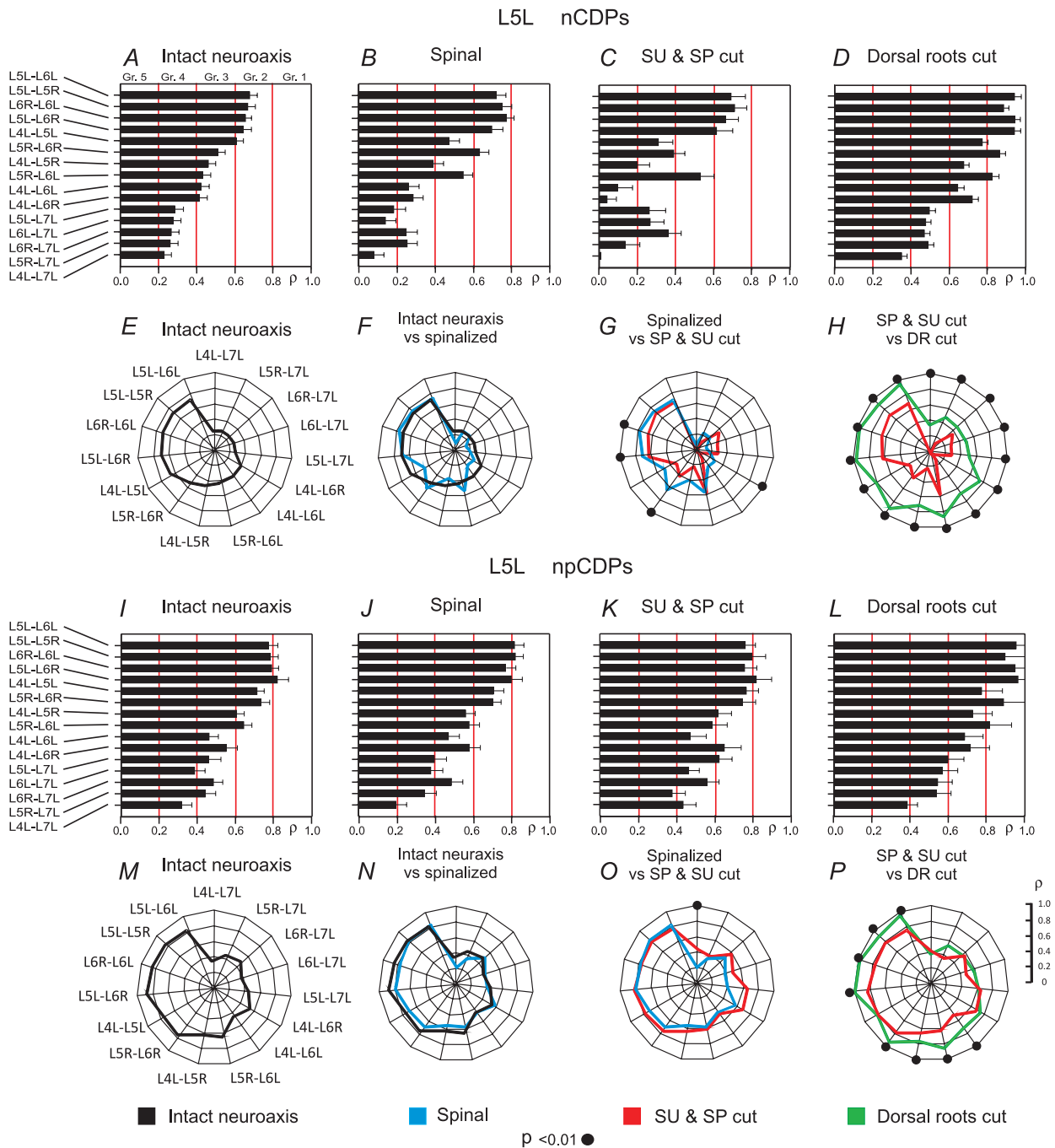
Figure 7. Effects of spinalization and deafferentation on the correlation between paired sets of spontaneous nCDPs and npCDPs retrieved using as reference the L5L CDPs

A, preparation with intact neuroaxis. Abscissa, coefficient of correlation (ρ) between paired sets of CDPs retrieved using as reference the L5L nCDPs. Horizontal bars show medians of coefficients arranged in decreasing order and their standard errors. Ordinates show different combinations of CDP recording sites. *E*, polar graph constructed with the medians of the coefficients of correlation displayed in *A*. *B* and *F*, the same but after acute spinalization. Polar graph shows superposed plots of data obtained from the preparation with intact neuroaxis (black) and of data obtained after spinalization (blue). *C* and *G* same after the acute section of the SU and SP nerves. Polar graph shows superposed plots of data obtained from the spinal preparation (blue) and after SU and SP nerve section (red). *D* and *H* after bilateral section of dorsal roots. Polar graph shows superposed plots of data obtained after SU and SP nerve section (red) and after dorsal root section (green). *I–P*, same as *A–H* for data obtained using as reference the L5L npCDPs. All pairs of CDPs are arranged in same order as in *A*. Correlation calibration scale in *P* applies to all polar graphs. Black circles indicate statistical significance of differences in correlation between paired sets of CDPs ($P < 0.01$). Further explanations in text.

the differences between the two distributions, both graphs have been plotted together in Fig. 9*A*. It may be seen that most of the npCDPs retrieved using as reference the L5L CDPs had a significantly higher correlation than

the nCDPs, as it was assessed performing a Wilcoxon test (see small circles around the polar plot). A similar tendency was observed for nCDPs and npCDPs retrieved using as reference the L6L CDPs (Fig. 8*A* and *I*), but
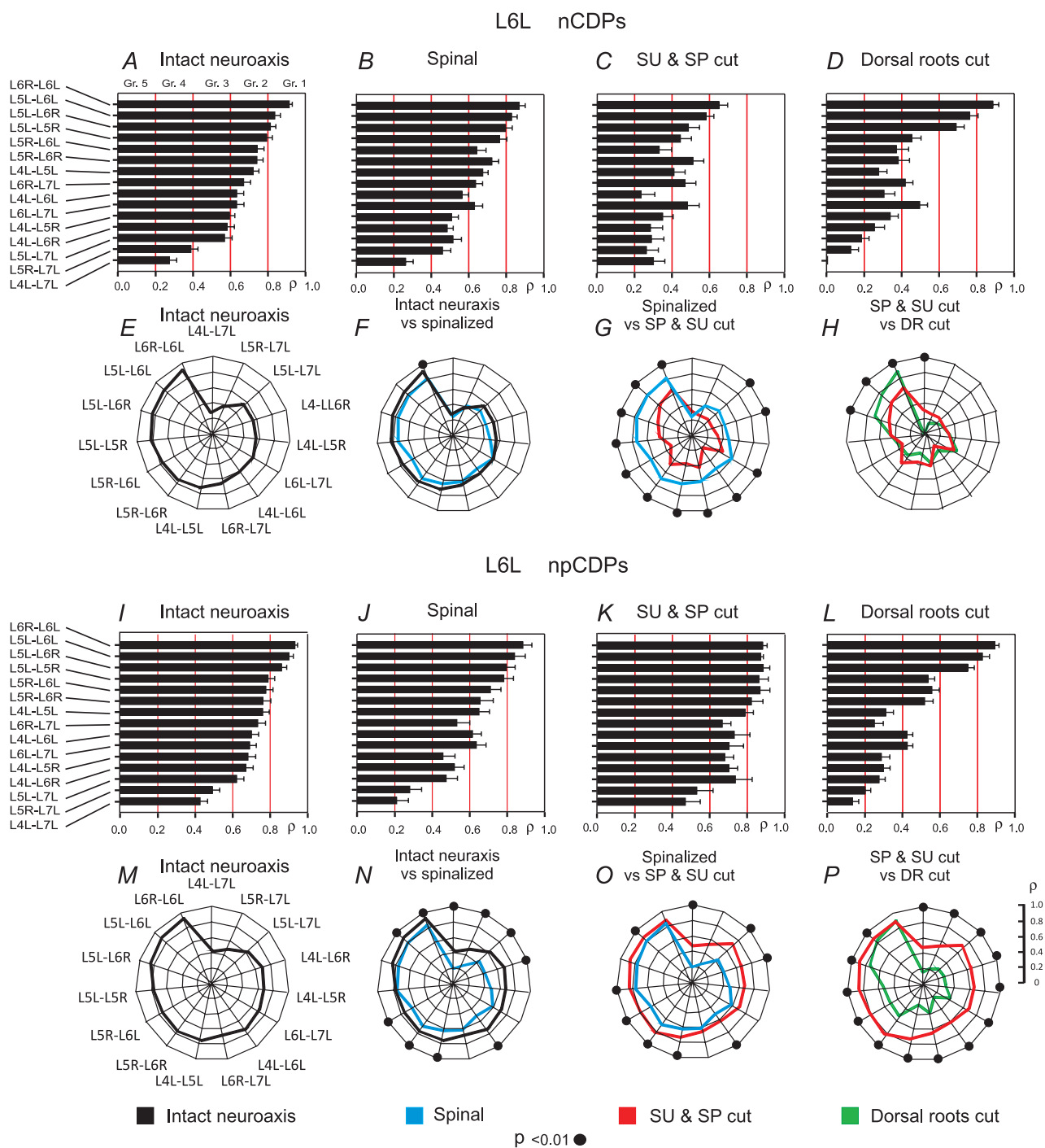

Figure 8. Effects of spinalization and deafferentation on correlation between paired sets of spontaneous nCDPs and npCDPs retrieved using as reference the L6L CDPs
Same format and experiment as in Fig. 7 but for CDPs retrieved using as reference the L6L nCDPs and npCDPs. In all cases coefficients of correlation were arranged according to the ranking order of the coefficients displayed in *A*, Further explanations in text.

the differences were smaller and not always statistically significant (Figs 8*E* and *M* and 9*E*).

Figure 10*A–C* displays data obtained in another experiment. In this case the intersegmental correlation between nCDPs and between npCDPs retrieved using as reference the L5L CDPs was in general higher than the correlation of the CDPs retrieved using as reference the L6L CDPs. For a given pair of recording sites, the differences in the correlation between paired sets of nCDPs and of pairs of npCDPs were rather small in comparison with those illustrated in the experiment of Fig. 9*A* and *E*.

These observations indicate that the magnitude of correlation between paired sets of CDPs depends not only on the segmental location of the reference CDPs (L5L or L6L), but also varies from one experiment to the other, probably because of differences in the state of the preparation (e.g. anaesthetic level). It is not clear, however, if the distributions of CDPs obtained by using as reference the CDPs generated in different segments involve the same or different sets of neurones (see Discussion). But even so, it should be stressed that in many cases, as in the experiment of Figs 6–9, the intersegmental correlation between spontaneous npCDPs was clearly higher than the correlation of the nCDPs, in agreement with our working hypothesis. Some of the functional implications of this finding are examined in the Discussion.

Effects of acute spinalization

We hypothesized that the patterns of segmental synchronization of the spontaneous nCDPs and npCDPs observed in anaesthetized preparations with intact neuro-axis largely result from the intrinsic organization of the spinal neuronal networks generating these potentials, which are modulated both by descending and by segmental activity. To evaluate the contribution of supraspinal influences, in three experiments we examined the effects of acute spinalization on the correlation between paired sets of spontaneous nCDPs and npCDPs recorded from different pairs of lumbo-sacral segments.

In the experiment of Fig. 6, sectioning the spinal cord at low thoracic level (T10), slightly reduced the mean amplitude of the spontaneous CDPs recorded in different segments relative to the mean amplitude of the reference CDPs. For example, the mean amplitude of the associated L5L and L4L nCDPs was reduced from 1.02 and 0.43 relative to the amplitude of the reference L6L nCDPs to 0.84 and 0.32, respectively. The coupling ratios of the associated nCDPs recorded from the right side (L6R and L5R) were less affected (from 1.08 and 0.49 to 0.96 and 0.46, respectively).

The intrasegmental correlation between paired sets of nCDPs and npCDPs retrieved using as reference the L5L and L6L CDPs was also reduced by spinalization, but these effects were barely significant (Figs 7F and N and 8*F* and N). Spinalization had also a relatively small effect on the correlation between npCDPs relative to the correlation of the nCDPs (Fig. 9*B* and *F*), but even so, the ranking order in the coefficients of correlation observed in the preparation with intact neuroaxis remained basically the same (Figs 7B and J and 8*B* and *J*). Similar results were observed in three experiments.

Altogether, these results indicate that in the anaesthetized preparation, descending influences slightly facilitate the activity of the neuronal networks involved in the generation of the CDPs and introduce a weak correlation on the neuronal networks involved in the generation of the nCDPs and npCDPs, mainly on those retrieved using as reference the L6L CDPs, but are not the main contributors to the intersegmental correlation between the CDPs.

Effects of acute section of cutaneous nerves and of dorsal roots

In a series of elegant studies on the functional organization of nociceptive withdrawal reflexes in the cat, Schouenborg and collaborators (1990, 1992) showed that the segmental projections of cutaneous afferents introduce a patterned activation of motoneurones that is probably mediated by the dorsal horn neuronal ensembles receiving the cutaneous inputs. We have shown previously that a significant fraction of the dorsal horn neurones that discharge in synchrony during the spontaneous CDPs respond mono- or oligosynaptically to electrical stimulation of low threshold afferents of the SU and of the SP nerves (Manjarrez *et al.* 2000; Contreras *et al.* 2010). Therefore it seemed possible that activity in low threshold cutaneous afferents contributed to the intersegmental correlation between the dorsal horn neurones involved in the generation of the CDPs. Hence, we hypothesized that in contrast with the relatively small action of descending pathways observed in the anaesthetized preparations, the acute section of the SU and SP nerves would have a significant influence on the intersegmental synchronization between paired sets of nCDPs and npCDPs.

In the spinal preparation, the acute transection of the left SU and SP nerves had relatively small effects on the mean amplitude of the CDPs. For example, in the experiment illustrated in Fig. 6, spinalization reduced the coupling ratio of the L5L CDPs from 1.02 to 0.84 relative to the reference L6L nCDPs that was increased to 0.97 after transection of the SU and SP nerves (see Fig. 6*B–D*). The coupling ratio of the L6R nCDPs relative to the L6L nCDPs reference potentials was reduced from 1.08 to 0.96 by spinalization and to 0.78 by SU and SP nerve section. The coupling ratio of the L5R nCDPs

relative to the reference L6L nCDPs remained basically unchanged by the spinalization and by the additional section of the SU and SP nerves (from 0.49 to 0.46 and 0.45, respectively).

The acute transection of the SU and SP nerves in the spinal preparation had rather small effects on the coefficient of correlation of the CDPs retrieved using as reference either the L5L nCDPs (Fig. 7*C* and *G*) or the L5L npCDPs (Fig. 7*K* and *O*). Nevertheless, the correlation between paired sets of nCDPs appeared to be significantly smaller than the correlation between the npCDPs (Fig. 9*C*). The differential effects produced by SU and SP nerve section on the correlation between paired sets of nCDPs and the npCDPs were more evident when using as reference the L6L CDPs (Fig. 9*G*) because in this case SU and SP nerve section reduced the correlation between nCDPs (see Fig. 8*C* and *G*) and increased the correlation between npCDPs (see Fig. 8*K* and *O*). Quite interestingly, in addition to the effects on the inter-segmental distribution of the correlation between pairs of CDPs, there was a clear disruption in their ranking order, that was more evident for the nCDPs than for the npCDPs (see Figs 7 and 8*C* and *K*).

The additional bilateral section of the dorsal roots increased the correlation of most CDPs selected using as reference the L5L nCDPs and npCDPs (Fig. 7*H* and *P*). The correlation between some of the paired sets of CDPs retrieved using as reference the L6L nCDPs was also increased (Fig. 8*H*), but in this case there was a clear reduction of the correlation between the CDPs retrieved by using as reference the L6L npCDPs (Fig. 8*P*). The differences in the intersegmental correlation between pairs of nCDPs and pairs of npCDPs induced by SU and SP nerve section were no longer observed following the bilateral section of the dorsal roots (Fig. 9*D* and *H*).

We also examined the effects produced by progressive deafferentation in preparations with intact neuroaxis. In the experiment of Fig. 10, sectioning the SU and SP nerves produced no significant changes in the coupling ratios of the mean CDPs disclosed by using as reference the L6L nCDPs (Fig. 10*A* and *D*). Yet, as in the spinal preparation, this procedure also had differential effects on the correlation between paired sets of nCDPs and npCDPs, particularly when using as reference the L6L CDPs (Fig. 10*E* and *F*). Sectioning the left sciatic nerve (Fig. 10*G–I*) and the dorsal roots
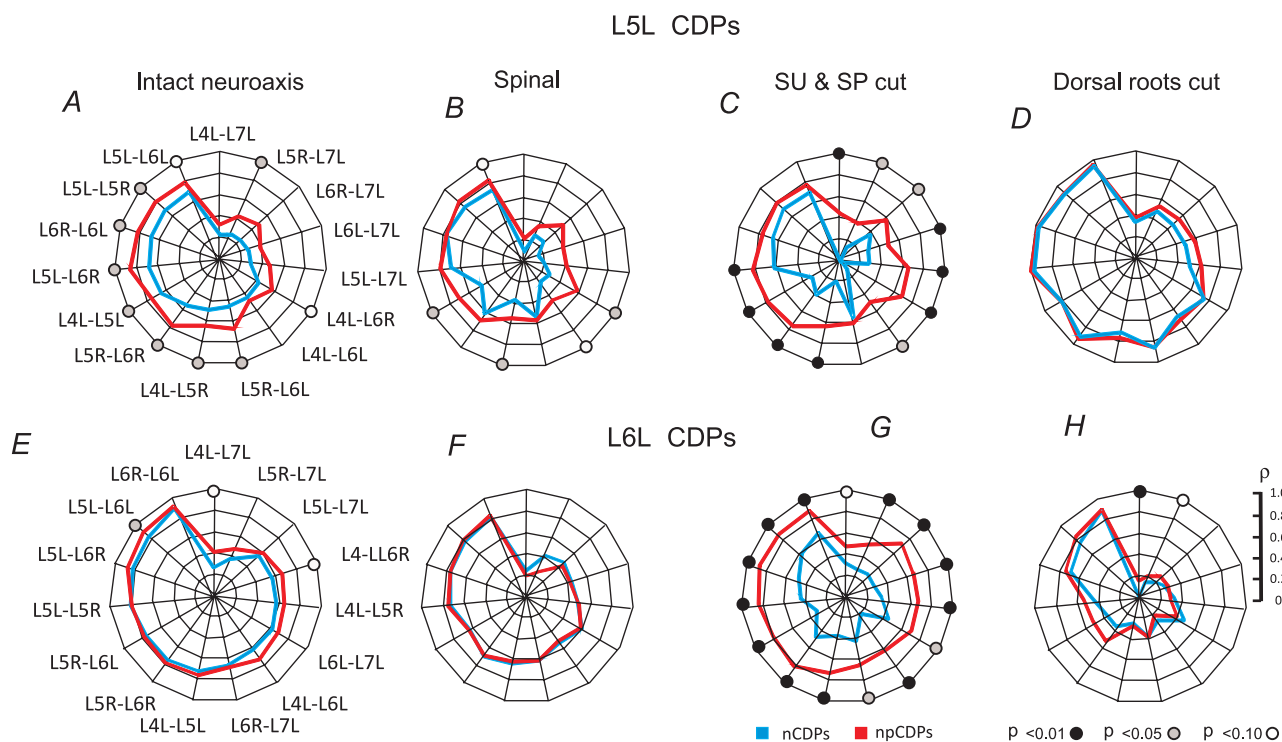

Figure 9. Effects of SU and SP nerve section on the intersegmental correlation of spontaneous nCDPs and of npCDPs
Same experiment as that of Figs 6–8. *A–D*, superposed polar graphs of intersegmental correlation between paired sets of CDPs retrieved using as reference the L5L nCDPs (blue) and npCDPs (red). *E–H*, same as *A–D* for potentials retrieved using as reference the L6L CDPs. Statistical significance of differences between the coefficients of correlation of nCDPs and npCDPs are indicated by circles (*P* < 0.01, black; *P* < 0.05, grey; and *P* < 0.10, white). Further explanations in text.

(Fig. 10*J–L*) increased the overall correlation between paired sets of nCDPs and of npCDPs and at the same time abolished the differential effects produced by SP and SU nerve section. Similar results were obtained in two other experiments.

Altogether, these observations indicate that the information conveyed by cutaneous nerves has a relevant role in the shaping of the intersegmental correlation between the neuronal ensembles involved in the generation of the spontaneous nCDPs and npCDPs. This modulation varies with the segmental location of

the neuronal networks involved in the generation of the CDPs.

Discussion

Characterization of the spontaneous CDPs in the lumbar spinal cord

In a previous study we used spike triggered averaging to disclose the possible connections of single interneurones with pathways producing PAD and postsynaptic inhibition
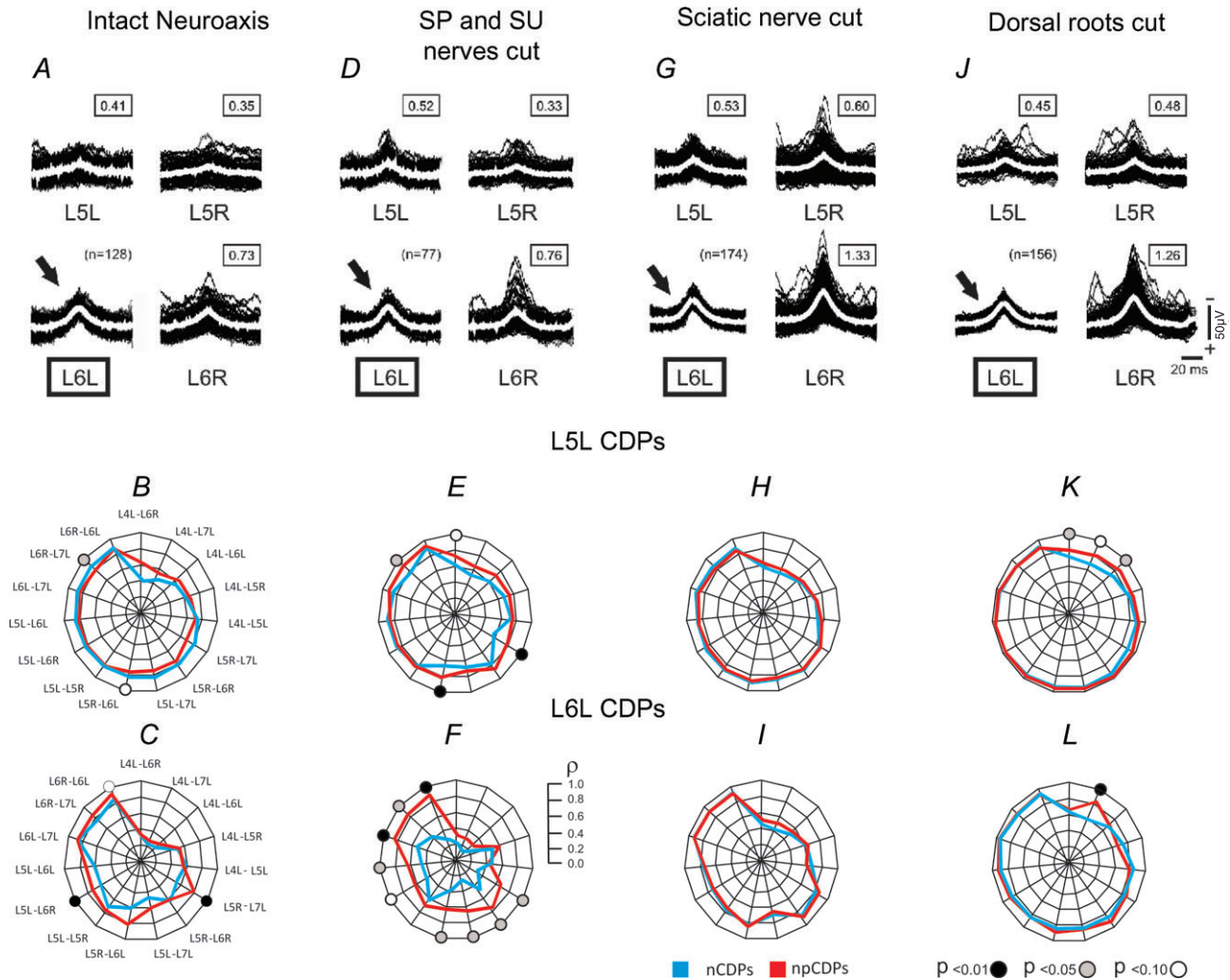

Figure 10. Effects of graded acute deafferentation on spontaneous CDPs in a preparation with intact neuroaxis

A, CDPs retrieved using as reference L6L nCDPs (see arrow). Neuroaxis and peripheral nerves intact. *B* and *C*, superposed polar plots of coefficients of correlation of paired sets of potentials recorded at different locations using as reference the L5L and L6L nCDPs (blue) and npCDPs (red). Coefficients of correlation calculated with data partly shown in *A*. *D–F*, recordings and polar plots made 20 min after the acute section of the left SP and SU nerves. *G–I*, same after the acute section of the left sciatic nerve made 40 min after the SU and SP nerve section. *J–L*, same after bilateral section of the L4–L7 dorsal roots made 45 min after sectioning the left sciatic nerve. Boxes in *A*, *D*, *G* and *J* show amplitude ratios of mean peak amplitudes of CDPs relative to peak amplitude of reference CDPs. Number of samples is shown in parentheses. Statistical significance of differences between the coefficients of correlation of nCDPs and npCDPs are indicated by circles ($P < 0.01$, black; $P < 0.05$, grey; and $P < 0.10$, white). Further explanations in text.

in spinal motoneurones (Rudomin *et al.* 1987). It soon became clear that the action potentials of many of the neurones located in the intermediate zone were preceded by slow negative CDPs. This raised the possibility that the examined interneurones were driven by dorsal horn neurones. Subsequent studies showed that these spontaneous CDPs appeared synchronized along several spinal segments, but there was little information on the functional organization of the neuronal networks mediating this synchronization (Manjarrez *et al.* 2003).

In contrast with our previous study, where the spontaneous CDPs were selected by amplitude discrimination (Manjarrez *et al.* 2003), the present set of observations was instead concerned with the analysis of two specific types of spontaneous CDPs: the nCDPs and npCDPs. These potentials were retrieved using predetermined templates with a ±20–30% range, under the assumption that this process would provide means to analyse the functional organization of the neurones involved in the generation of relatively homogeneous sets of CDPs.

We have found that the neurones associated with the generation of the spontaneous nCDPs and npCDPs are located within the dorsal horn in Rexed's laminae III and IV, mostly in segments L5 and L6, in the same intraspinal regions where the low threshold SU and SP afferents project (Fig. 5).

Our observations also indicate that the nCDPs and npCDPs recorded from different spinal segments remain highly synchronized in the spinal and deafferented preparation (Fig. 9*D* and *H* and Fig. 10*K* and *L*). This suggests that the basic patterns of intersegmental synchronization are generated by intrinsic spinal mechanisms, that is by the interconnections between particular groups of dorsal horn neurones distributed along the lumbo-sacral segments. The changes in correlation observed after sectioning the SU and SP further indicate that the signals conveyed by these nerves play an important role in shaping the patterns of intersegmental correlation between the different sets of dorsal horn neurones. Most likely, the synchronization between the nCDPs and npCDPs generated in different segments is mediated by neurones connected with other neurones in the same and in opposite sides of the spinal cord, among them the commissural interneurones (Bannatyne *et al.* 2003; Jankowska *et al.* 2007, 2009). Our observations also emphasize the complexity of the local interconnections between these neuronal networks.

The larger and smaller CDPs excluded from the selection procedure could be generated by neuronal populations different from those producing the template-selected CDPs. Neurones located within the most superficial layers in the dorsal horn (Rexed's laminae I and II) are known to fire in synchrony with the spontaneous DRPs (Lidierth & Wall, 1998) and could well contribute to the generation of the relatively small CDPs

associated with the spontaneous nCDPs and npCDPs (see below). Pertaining to the large 'unselected' CDPs, it seems likely they are produced by the same sets of neurones that generate the mid-sized CDPs retrieved with the templates, but this remains to be tested.

Are the nCDPs and npCDPs generated by the same or by different sets of dorsal horn neurones?

The finding that the spontaneous DRPs, which are a sign of PAD, are preferentially associated with the npCDPs (Fig. 4) could suggest that separate sets of dorsal horn neurones are involved in the generation of the spontaneous nCDPs and npCDPs. However, an alternative possibility would be that the negative components of both the nCDPs and the npCDPs are generated by the same set of dorsal horn neurones in Rexed's laminae III and IV, as suggested by the contour plots depicted in Fig. 5*E* and *F*. Under conditions of weak activation and/or low synchronization, this set of neurones would generate the nCDPs and activate the Class I interneurones mediating the non-reciprocal Ib inhibition. Increased neuronal activation and/or increased synchronization between the spontaneous activity of this set of neurones would generate a more effective excitatory drive and recruit the pathways producing PAD of cutaneous afferents in the dorsal horn and of muscle afferents, possibly via Class II interneurones in the intermediate zone. The activation of Class I intermediate zone interneurones without concurrent generation of DRPs observed by Rudomin *et al.* (1987) could result from reciprocal inhibitory interactions between Class I and Class II interneurones within the intermediate zone, but this issue remains to be investigated.

The contribution of increased synchronization to the recruitment of the pathways leading to PAD is supported by the finding that the coefficient of correlation between pairs of npCDPs was often higher than the coefficient between the nCDPs (see Fig. 9*A* and *E*), particularly after transecting the SU and SP nerves (Fig. 9*C* and *G*). The need of spatial and temporal summation to produce a significant PAD, particularly in the case of muscle afferents, has been documented some time ago (Eccles *et al.* 1962*a,b,c*).

Additional support for this possibility is provided by the recent findings of Contreras *et al.* (2010) who examined in the anaesthetized cat the temporal relationship of the activity of single L6 dorsal horn neurones located in Rexed's laminae III–IV with the spontaneous nCDPs and npCDPs. They found that 44% of the examined neurones increased their spontaneous firing rate during both the L6 nCDPs and npCDPs. On several occasions the same micropipette recorded the activity of pairs of neurones that fired in synchrony with both types of CDPs. In those cases the probabilities of neuronal joint firing were higher

during the npCDPs that during the nCDPs. There was also a smaller fraction of neurones (20%) that increased their firing rate only during the nCDPs and an even smaller fraction (4%) that discharged only during the npCDPs.

Functional organization of the dorsal horn neurones involved in the generation of the nCDPs and npCDPs

The observations presented here, albeit limited, support the notion that the spontaneous nCDPs and npCDPs result from the activation of segmental sets of dorsal horn neuronal aggregates distributed along several lumbo-sacral segments (for intermediate zone interneurones see Jankowska & Edgley, 2010). The intersegmental connections between these neuronal aggregates appear not to be random, but have an intrinsic organization (see Fig. 3) that is partly disrupted following deafferentation, as illustrated in Figs 7 and 8. It is not clear, however, if these neuronal aggregates have a stereotyped (modular) structure as proposed by Saltiel *et al.* (1998), Tresch & Bizzi (1999) and Lemay & Grill (2004) for spinal neurones interspersed throughout the grey matter, mostly concentrated in laminae III–IV, or alternatively, as suggested by the present set of observations, each set of neurones is able to express different patterns, depending on the overall balance between excitatory and inhibitory inputs received at that time.

Clearly, this issue requires identification of the neurones involved in the generation of the spontaneous nCDPs and npCDPs and a more detailed characterization of their responses to sensory and supraspinal inputs as well as of their interconnections with other neurones (see above). There are several studies on the correlation between the spontaneous activity of different sets of dorsal horn neurones and how it is modified by nociceptive stimulation, but they provide limited information pertaining to their participation in the generation of the spontaneous CDPs analysed at present (Sandkuhler & Eblen-Zajjur, 1994; Sandkuhler *et al.* 1995; Biella *et al.* 1997; Galhardo *et al.* 2002; Eichler *et al.* 2003).

Comparison with other studies

Previous studies support the notion that last order interneurones mediating the PAD of group Ia and Ib afferents are located within the intermediate zone, in contrast with the last order interneurones producing PAD of cutaneous afferents, which are located in the dorsal horn (Jankowska *et al.* 1981; Rudomin *et al.* 1987). In line with our previous proposals, the present series of observations indicates that the neurones producing the npCDPs, which are preferentially associated with spontaneous DRPs and respond to stimulation of low threshold afferents, are located in the

deeper layers of the dorsal horn, namely in Rexed's layers III and IV.

At first glance, these findings seem to present a discrepancy with those of Lidierth & Wall (1998) in the rat spinal cord, who proposed that neurones in the Lissauer tract mediate the PAD of cutaneous afferents and contribute to the intersegmental synchronization of spontaneous DRPs. However, this may not be the case for the generation of the spontaneous nCDPs and npCDPs in the cat spinal cord because, as shown in Fig. 4, the DRPs are preferentially associated with the spontaneous npCDPs, most likely generated by interneurones located deeper in the dorsal horn, in Rexed's laminae III and IV (Fig. 5). Nevertheless, it is possible that the superficial and deeper sets of dorsal horn neurones produce PAD in different groups of afferent fibres, a situation resembling that of group II afferents where there is a differential control of presynaptic inhibition affecting transmission from these afferents to neurones in the dorsal horn and in the intermediate zone (Jankowska *et al.* 2002). Studies of PAD patterns in pairs of collaterals of single cutaneous afferents projecting to different regions within the dorsal horn could probably help to clarify this situation.

Some functional considerations

The relevance of temporal synchronization as an effective way to activate alternative synaptic pathways has been emphasized by several investigators and is considered as an important control mechanism in the execution of a variety of sensory and motor tasks (see Konig *et al.* 1995; Womelsdorf & Fries, 2006; Womelsdorf *et al.* 2007). The present series of observations supports the proposal that increased synchronization between the dorsal horn neurones involved in the generation of the nCDPs may recruit the pathways mediating PAD and generate the npCDPs. This may allow the activation of specific neuronal aggregates with precise roles in the motor and sensory domain (Rudomin *et al.* 1975; Lomelí *et al.* 1998; Rudomin & Schmidt, 1999) and could function as an efficient mechanism to remove undesired information arriving from cutaneous afferents during active muscle contraction as shown in behaving monkeys by Seki *et al.* (2003), as well as during different stages in locomotion (Rossignol & Beloozerova, 1998; Beloozerova & Rossignol, 2004). This control of sensory information could contribute to the development of a higher coherence between the programmed and the executed voluntary movements (Georgopoulos, 1995) and also contribute to the spatial and temporal sharpening of sensory information (Rudomin & Schmidt, 1999).

In this regard, an unexpected finding was that sectioning the SU and SP nerves reduced the correlation between the spontaneous nCDPs while at the same time increasing the

correlation between the spontaneous npCDPs. Reduced correlation between the nCDPs would allow a more independent and perhaps more selective control of the tonic Ib actions exerted on a variety of spinal pathways, while increased correlation between the npCDPs would produce a more synchronous and perhaps widespread presynaptic modulation of the synaptic actions of sensory fibres (Rudomin & Madrid, 1972; Rudomin *et al.* 1975).

The acute section of a cutaneous nerve not only reduces the sensory input to the spinal cord, but also induces a state of central sensitization (Sandkuhler, 2000) that unmasks the responses of dorsal horn neurones to activation of cutaneous afferents (Biella & Sotgiu, 1995) and changes the tonic PAD of these afferents in a history dependent manner, as suggested by the observations of García *et al.* (2007, 2008) and of Rudomin (2009). State dependent changes of the functional connectivity between the neuronal ensembles involved in the generation of the spontaneous CDPs may also change the context of the information transmitted by the ensemble, as suggested by the recent findings of Lam *et al.* (2008) and Gibson *et al.* (2009), and underscores the need for developing non-invasive methods to analyse the changes in the functional organization of the spontaneous CDPs and of the associated dorsal horn neurones both in experimental animals and in patients under conditions that involve significant alterations of spinal interneuronal activity (Crone *et al.* 1994; Morita *et al.* 2000, 2001; Orsnes *et al.* 2000; Salazar-Torres *et al.* 2004; Knikou, 2005; Chu *et al.* 2009).

One question that remains to be answered is the extent to which the neurones involved in the generation of the spontaneous nCDPs and npCDPs analysed at present are also rhythmically active during scratching and/or during fictive locomotion. In view of the recent report of Cuellar *et al.* (2010) this seems not to be the case. These investigators found in the decerebrate cat some dorsal horn interneurones with bursting activity time locked to spontaneous nCDPs that were not rhythmically active during scratching (Cuellar *et al.* 2009). They also found other neurones that fired rhythmically during the flexor or extensor phases of scratching, but were not synchronized with the spontaneous nCDPs. Yet, these observations need to be taken with caution because, as discussed above, the 'state' of the preparation may also determine the activation of alternative spinal pathways (Perreault *et al.* 1999; Hultborn, 2001; Stecina *et al.* 2005). It is therefore possible that the sets of dorsal horn neurones involved in the generation of the spontaneous nCDPs and npCDPs are involved in other types of behaviour, not only locomotion.

Concluding remarks

The present observations are consistent with the proposal that the spinal neuronal ensembles involved in the generation of the spontaneous nCDPs and npCDPs are organized as a dynamic network of interconnected sets bilaterally distributed along the lumbo-sacral segments. As a consequence of their intrinsic organization, these sets of neurones fire synchronously giving rise to a variety of activation patterns which can be modified by segmental and descending influences. The extensive inter-connectivity between these neuronal networks explains, to some extent, the inability of lesions confined to one side of the spinal cord to completely desynchronize the nCDPs and npCDPs recorded from the segments separated by the lesion (Rodríguez *et al.* 2010, 2011). An interesting feature of these networks is that low temporal synchronization in neuronal firing allows a relatively independent and perhaps selective activation of the pathways mediating the Ib non-reciprocal postsynaptic inhibition exerted on different sets of motoneurones, while increased synchronization within these networks allows the alternate, coherent activation of pathways mediating PAD and presynaptic inhibition. This 'state-dependent' selection of alternate spinal pathways could play a significant role in the execution of a variety of sensory and motor tasks.

References

Bannatyne BA, Edgley SA, Hammar I, Jankowska E & Maxwell DJ (2003). Networks of inhibitory and excitatory commissural interneurones mediating crossed reticulospinal actions. *Eur J Neurosci* **18**, 2273–2284.

Beloozerova IN & Rossignol S (2004). Antidromic discharges in dorsal roots of decerebrate cats. II: Studies during treadmill locomotion. *Brain Res* **996**, 227–236.

Biella G, Riva L & Sotgiu ML (1997). Interaction between neurones in different laminae of the dorsal horn of the spinal cord. A correlation study in normal and neuropathic rats. *Eur J Neurosci* **9**, 1017–1025.

Biella G & Sotgiu ML (1995). Evidence that inhibitory mechanisms mask inappropriate somatotopic connections in the spinal cord of normal rat. *J Neurophysiol* **74**, 495–505.

Chu J, Wagle-Shukla A, Gunraj C, Lang AE & Chen R (2009). Impaired presynaptic inhibition in the motor cortex in Parkinson disease. *Neurology* **72**, 842–849.

Crone C, Nielsen J, Petersen N, Ballegaard M & Hultborn H (1994). Disynaptic reciprocal inhibition of ankle extensors in spastic patients. *Brain* **117**, 1161–1168.

Contreras-Hernández E, Chávez D & Rudomin P (2010). Increased synchronization of dorsal horn neuronal activity releases presynaptic inhibitory pathways. *2010 Abstract Viewer/Itinerary Planner*, Programme No. 286.20. Society for Neuroscience, Washington, DC.

Cuellar C, Tapia JA, Trejo A, Delgado-Lezama R, Gutiérrez R, Jiménez I, Rudomin P & Manjarrez E (2010). Dorsal horn interneurones bursting in synchrony with spontaneous cord dorsum potentials are not rhythmically active during fictive scratching. *2010 Abstract Viewer/Itinerary Planner*, Programme No. 783.15. Society for Neuroscience, Washington, DC.

Cuellar CA, Tapia JA, Juárez V, Quevedo J, Linares P, Martínez L & Manjarrez E (2009). Propagation of sinusoidal electrical waves along the spinal cord during a fictive motor task. *J Neurosci* **29**, 798–810.

Drummond GB (2009). Reporting ethical matters in *The Journal of Physiology*: standards and advice. *J Physiol* **587**, 713–719.

Eccles JC, Kostyuk PG & Schmidt RF (1962*a*). Central pathways responsible for depolarization of primary afferent fibres. *J Physiol* **161**, 237–257.

Eccles JC, Magni F & Willis WD (1962*b*). Depolarization of central terminals of group I afferent fibres from muscle. *J Physiol* **160**, 62–93.

Eccles JC, Schmidt RF & Willis WD (1962*c*). Presynaptic inhibition of the spinal monosynaptic reflex pathway. *J Physiol* **161**, 282–297.

Eccles JC (1963). Depolarization of the central terminals of cutaneous afferent fibres. *J Neurophysiol* **26**, 646–661.

Eichler M, Dahlhaus R & Sandkuhler J (2003). Partial correlation analysis for the identification of synaptic connections. *Biol Cybern* **89**, 289–302.

Galhardo V, Apkarian AV & Lima D (2002). Peripheral inflammation increases the functional coherency of spinal responses to tactile but not nociceptive stimulation. *J Neurophysiol* **88**, 2096–2103.

García CA, Chávez D, Jiménez I & Rudomin P (2007). Resetting of tonic PAD by acute section of cutaneous nerves. *2007 Abstract Viewer/Itinerary Planner*, Programme No. 77.13. Society for Neuroscience, Washington, DC.

García CA, Chávez D, Jiménez I & Rudomin P (2008). The unmasking phenomenon in chronically crushed cutaneous afferents: plasticity of PAD pathways. *2008 Abstract Viewer/Itinerary Planner*, Programme No. 73.14. Society for Neuroscience, Washington, DC.

García CA, Chávez D, Jiménez I & Rudomin P (2004). Effects of spinal and peripheral nerve lesions on the intersegmental synchronization of the spontaneous activity of dorsal horn neurones in the cat lumbo-sacral spinal cord. *Neurosci Lett* **361**, 102–105.

Georgopoulos AP (1995). Current issues in directional motor control. *Trends Neurosci* **18**, 506–510.

Gibson W, Arendt-Nielsen L, Sessle BJ & Graven-Nielsen T (2009). Glutamate and capsaicin-induced pain, hyperalgesia and modulatory interactions in human tendon tissue. *Exp Brain Res* **194**, 173–182.

Hultborn H (2001). State-dependent modulation of sensory feedback. *J Physiol* **533**, 5–13.

Jankowska E & Edgley SA (2010). Functional subdivision of feline spinal interneurones in reflex pathways from group Ib and II muscle afferents; an update. *Eur J Neurosc* **32**, 881–893.

Jankowska E, Bannatyne BA, Stecina K, Hammar I, Cabaj A & Maxwell DJ (2009). Commissural interneurones with input from group I and II muscle afferents in feline lumbar segments: neurotransmitters, projections and target cells. *J Physiol* **587**, 401–418.

Jankowska E, Maxwell DJ & Bannatyne BA (2007). On coupling and decoupling of spinal interneuronal networks. *Arch Ital Biol* **145**, 235–250.

Jankowska E, McCrea D, Rudomin P & Sykova E (1981). Observations on neuronal pathways subserving primary afferent depolarization. *J Neurophysiol* **46**, 506–516.

Jankowska E, Slawinska U & Hammar I (2002). Differential presynaptic inhibition of actions of group II afferents in di- and polysynaptic pathways to feline motoneurones. *J Physiol* **542**, 287–299.

Kerkut BA & Bagust J (1995). The isolated mammalian spinal cord. *Prog Neurobiol* **46**, 1–48.

Knikou M (2005). Effects of hip joint angle changes on intersegmental spinal coupling in human spinal cord injury. *Exp Brain Res* **167**, 381–393.

Konig P, Engel AK, Roelfsema PR & Singer W (1995). How precise is neuronal synchronization? *Neural Comput* **7**, 469–485.

Lam DK, Sessle BJ & Hu JW (2008). Surgical incision can alter capsaicin-induced central sensitization in rat brainstem nociceptive neurones. *Neurosc* **156**, 737–747.

Lemay MA & Grill WM (2004). Modularity of motor output evoked by intraspinal microstimulation in cats. *J Neurophysiol* **91**, 502–514.

Lidierth M & Wall PD (1996). Synchronous inherent oscillations of potentials within the rat lumbar spinal cord. *Neurosc Lett* **220**, 25–28.

Lidierth M & Wall PD (1998). Dorsal horn cells connected to the Lissauer tract and their relation to the dorsal root potential in the rat. *J Neurophysiol* **80**, 667–679.

Lomelí J, Quevedo J, Linares P & Rudomin P (1998). Local control of information flow in segmental and ascending collaterals of single afferents. *Nature* **395**, 600–604.

Manjarrez E, Jiménez I & Rudomin P (2003). Intersegmental synchronization of spontaneous activity of dorsal horn neurones in the cat spinal cord. *Exp Brain Res* **148**, 401–413.

Manjarrez E, Rojas-Piloni JG, Jiménez I & Rudomin P (2000). Modulation of synaptic transmission from segmental afferents by spontaneous activity of dorsal horn spinal neurones in the cat. *J Physiol* **529**, 445–460.

Morita H, Crone C, Christenhuis D, Petersen NT & Nielsen JB (2001). Modulation of presynaptic inhibition and disynaptic reciprocal Ia inhibition during voluntary movement in spasticity. *Brain* **124**, 826–837.

Morita H, Shindo M, Ikeda S & Yanagisawa N (2000). Decrease in presynaptic inhibition on heteronymous monosynaptic Ia terminals in patients with Parkinson's disease. *Mov Disord* **15**, 830–834.

National Research Council (2010) *Guide for the Care and Use of Laboratory Animals*, 8th edn The National Academic Press, Washington, DC.

Orsnes G, Crone C, Krarup C, Petersen N & Nielsen J (2000). The effect of baclofen on the transmission in spinal pathways in spastic multiple sclerosis patients. *Clin Neurophysiol* **111**, 1372–1379.

Perreault MC, Shefchyk SJ, Jiménez I & McCrea DA (1999). Depression of muscle and cutaneous afferent-evoked monosynaptic field potentials during fictive locomotion in the cat. *J Physiol* **521**, 691–703.

Rodríguez E, Chávez D, Hernández E & Rudomin P (2010). State dependent changes in the fractal structure of spontaneous cord dorsum potentials induced by peripheral nerve and spinal lesions in the anesthetized cat. *2010 Abstract Viewer/Itinerary Planner*, Programme No. 286.15. Society for Neuroscience, Washington, DC.

Rodríguez EE, Hernández-Lemus E, Itzá-Ortiz BA, Jiménez I & Rudomin P (2011) Multichannel detrended fluctuation analysis reveals synchronized patterns of spontaneous spinal activity in anesthetized cats. *PLoS ONE* **6**, e26449.

Rossignol S & Beloozerova IN (1998). Presynaptic mechanism during locomotion. In *Presynaptic Inhibition and Neural Control*, ed. Rudomin P, Romo R & Mendell LM, pp. 385–397. Oxford University Press, New York.

Rudomin P (1990). Presynaptic inhibition of muscle spindle and tendon organ afferents in the mammalian spinal cord. *Trends Neurosci* **13**, 499–505.

Rudomin P (2009). In search of lost presynaptic inhibition. *Exp Brain Res* **196**, 139–151.

Rudomin P, Burke RE, Núñez R, Madrid J, & Dutton H (1975). Control by presynaptic correlation: a mechanism affecting information transmission from Ia fibres to motoneurones. *J Neurophysiol* **38**, 267–284.

Rudomin P, Dutton H & Muñoz-Martínez J (1969). Changes in correlation between monosynaptic reflexes produced by conditioning afferent volleys. *J Neurophysiol* **32**, 759–772.

Rudomin P, Hernández E & Lomelí J (2007). Tonic and phasic differential GABAergic inhibition of synaptic actions of joint afferents in the cat. *Exp Brain Res* **176**, 98–118.

Rudomin P, Jiménez I, Quevedo J & Solodkin M (1990). Pharmacologic analysis of inhibition produced by last-order intermediate nucleus interneurones mediating nonreciprocal inhibition of motoneurones in cat spinal cord. *J Neurophysiol* **63**, 147–160.

Rudomin P & Madrid J (1972). Changes in correlation between monosynaptic responses of single motoneurones and in information transmission produced by conditioning volleys to cutaneous nerves. *J Neurophysiol* **35**, 44–64.

Rudomin P & Schmidt RF (1999). Presynaptic inhibition in the vertebrate spinal cord revisited. *Exp Brain Res* **129**, 1–37.

Rudomin P, Solodkin M & Jiménez I (1987). Synaptic potentials of primary afferent fibres and motoneurones evoked by single intermediate nucleus interneurones in the cat spinal cord. *J Neurophysiol* **57**, 1288–1313.

Salazar-Torres JJ, Pandyan AD, Price CI, Davidson RI, Barnes MP & Johnson GR (2004). Does spasticity result from hyperactive stretch reflexes? Preliminary findings from a stretch reflex characterization study. *Disabil Rehabil* **26**, 756–760.

Saltiel P, Tresch MC & Bizzi E (1998). Spinal cord modular organization and rhythm generation: an NMDA iontophoretic study in the frog. *J Neurophysiol* **80**, 2323–2339.

Sandkuhler J (2000). Learning and memory in pain pathways. *Pain* **88**, 113–118.

Sandkuhler J, Eblen-Zajjur A, Fu QG & Forster C (1995). Differential effects of spinalization on discharge patterns and discharge rates of simultaneously recorded nociceptive and non-nociceptive spinal dorsal horn neurones. *Pain* **60**, 55–65.

Sandkuhler J & Eblen-Zajjur AA (1994). Identification and characterization of rhythmic nociceptive and non-nociceptive spinal dorsal horn neurones in the rat. *Neurosci* **61**, 991–1006.

Schouenborg J, Holmberg H & Weng HR (1992). Functional organization of the nociceptive withdrawal reflexes. II. Changes of excitability and receptive fields after spinalization in the cat. *Exp Brain Res* **90**, 469–478.

Schouenborg J & Kalliomaki J (1990). Functional organization of the nociceptive withdrawal reflexes. I. Activation of hindlimb muscles in the rat. *Exp Brain Res* **83**, 67–78.

Seki K, Perlmutter SI & Fetz EE (2003). Sensory input to primate spinal cord is presynaptically inhibited during voluntary movement. *Nat Neurosci* **6**, 1309–1316.

Stecina K, Quevedo J & McCrea DA (2005). Parallel reflex pathways from flexor muscle afferents evoking resetting and flexion enhancement during fictive locomotion and scratch in the cat. *J Physiol* **569**, 275–290.

Tresch MC & Bizzi E (1999). Responses to spinal microstimulation in the chronically spinalized rat and their relationship to spinal systems activated by low threshold cutaneous stimulation. *Exp Brain Res* **129**, 401–416.

Wall PD & Werman R (1976). The physiology and anatomy of long ranging afferent fibres within the spinal cord. *J Physiol* **255**, 321–334.

Womelsdorf T & Fries P (2006). Neuronal coherence during selective attentional processing and sensory-motor integration. *J Physiol (Paris)* **100**, 182–193.

Womelsdorf T, Schoffelen JM, Oostenveld R, Singer W, Desimone R, Engel AK & Fries P (2007). Modulation of neuronal interactions through neuronal synchronization. *Science* **316**, 1609–1612.

Author contributions

Acknowledgements